The Q motif is involved in DNA binding that affects ATP hydrolysis and unwinding in ChlR1 helicase

A Thesis Submitted to the College of
Graduate Studies and Research
In Fulfillment of the Requirements
for the Degree of Master of Science
in the Department of Biochemistry
University of Saskatchewan
Saskatoon

By
Hao Ding

Permission of Use Statement

I hereby present this thesis in partial fulfilment of the requirements for a postgraduate degree from the University of Saskatchewan and agree that the Libraries of this University may make it freely available for inspection. I further agree that permission for copying of this thesis in any manner, either in whole or in part, for scholarly purposes may be granted by the professor or professors who supervised this thesis or, in their absence, by the Head of the Department or the Dean of the College in which my thesis work was done. It is understood that any copying or publication or use of this thesis or parts of it for any financial gain will not be allowed without my written permission. It is also understood that due recognition shall be given to me and to the University of Saskatchewan in any scholarly use which may be made of any material in my thesis.

Requests for permission to copy or to make other use of material in this thesis in whole or part should be addressed to:

Head of the Department of Biochemistry
University of Saskatchewan
107 Wiggins Road
Saskatoon, Saskatchewan,
Canada S7N 5E5

Abstract

Helicases are molecular motors that couple the energy of nucleoside triphosphate (NTP) hydrolysis to the unwinding and remodeling of structured DNA or RNA. The conversion of energy derived from NTP hydrolysis into unwinding of double-stranded nucleic acids is coordinated by seven sequence motifs (I, Ia, II, III, IV, V, and VI). The Q motif, consisting of an invariant glutamine (Q) residue, has been identified in some, but not all helicases. Compared with the seven well-recognized conserved helicase motifs, the role of the Q motif is not well known. Mutations in the human *ChlR1 (DDX11)* gene are associated with Warsaw Breakage Syndrome characterized by cellular defects in genome maintenance. ChlR1 is known to play essential roles to preserve genomic stability, particularly in sister chromatid cohesion. To examine the roles of the Q motif in the ChlR1 helicase, we performed site directed mutagenesis of glutamine to alanine at residue 23 in the Q motif of ChlR1. ChlR1 recombinant wild type (WT) and mutant (Q23A) proteins were overexpressed and purified from HEK293T cells. The ChlR1-Q23A mutant abolished the helicase activity of ChlR1, and displayed reduced DNA binding ability. The mutant showed impaired ATPase activity but displayed normal ATP binding. The Q motif in FANCJ helicase, a ChlR1 homolog, regulates FANCJ's dimerization, while our size exclusion chromatography (SEC) indicated that the ChlR1 protein functions as a monomer. A thermal shift assay revealed that ChlR1-Q23A has a similar melting point as ChlR1-WT. Partial proteolysis mapping demonstrated that ChlR1-WT and Q23A have similar globular structures, although there are some subtle conformational differences between these two proteins. Taken together, our results suggest that the Q motif in ChlR1 helicase is involved in DNA binding but not in ATP binding.

Acknowledgements

I wish to express my sincere thanks to my supervisor Dr. Yuliang Wu for his endless support on academic studies and his helpful guidance on my life. I take this opportunity to express gratitude to my committee member Dr. Jeremy Lee and Dr. Stanley Moore for their guidance and support throughout my project. I would also like to thank Dr. Linda Chelico (Department of Microbiology & Immunology) for teaching and assisting me on the steady-state fluorescence depolarization assay. I would like to thank everyone in Dr. Wu's lab for their support and encouragement, including Dr. Manhong Guo, Dr. Venkatasubramanian Vidhyasagar, Tanu Talwar, and Yujiong (John) He. I would like to thank all members of the Cancer Cluster, all graduates and faculty in the Department of Biochemistry. I am grateful to have had access to the Protein Characterization and Crystallization Facility (PCCF) of PRISM, particularly Dr. Michal Boniecki. I also thank my parents for the unceasing encouragement, support, and attention. I am also grateful to my friends who supported and encouraged me through my master's program.

Contents

List of Figures

List of Tables

List of Abbreviations

EMSA	Electrophoretic mobility shift assays
PAGE	Polyacrylamide gel electrophoresis
PEI	Polyethylenimine
SEC	Size exclusion chromatography
SF2	Superfamily 2
XPD	Xeroderma pigmentosum complementation group D
TaXPD	*Thermoplasma acidophilum* XPD
TLC	Thin-layer chromatography
TSA	Thermal stability shift assay
WABS	Warsaw Breakage Syndrom

1. Introduction

1.1 Helicases

The first helicase protein was discovered in *Escherichia coli* (Abdel-Monem *et al*., 1976) and then helicases with diverse functions have been found in all organisms. The number of helicases expressed in higher organisms is strikingly high, with approximately 1% of the genes in many eukaryotic genomes. Helicases are motor proteins that move directionally along a nucleic acid phosphodiester backbone, separating two annealed nucleic acid strands (i.e., DNA, RNA, or DNA-RNA hybrid) using energy derived from ATP hydrolysis. Helicases can be classified into 5'→3' helicases or 3'→5' helicases based on their direction of movement. According to their substrates, helicases are classified into DNA and RNA helicases, although some can function on both DNA and RNA molecules (Pyle, 2008).

Helicases play roles in virtually all aspects of nucleic acid metabolism, including replication, repair, recombination, transcription, chromosome segregation, and telomere maintenance, ribosome biogenesis, mRNA splicing, and mitochondrial RNA processing (Brosh, Jr. and Bohr, 2007; Lohman and Bjornson, 1996; Tanner and Linder, 2001). DNA helicases have been reported to function in a variety of DNA metabolic processes, including unwinding duplex and alternative DNA structures (triplex, G-quadruplex), displacing protein bound to DNA, and chromatin remodeling *(*Bernstein *et al.*, 2010*;* Dillingham, 2011*;* Singh *et al*., 2012). RNAs can also fold into specific three-dimensional structures that include secondary (RNA helices) and tertiary structure and bind with ribonucleoprotein complexes (RNPs) where unwinding and remodeling are required in which RNA helicase plays a vital role (Jankowsky, 2011). RNA helicases are also essential for RNA metabolism like mRNA splicing, transcription, RNA editing, RNA export, rRNA processing, RNA degradation, and regulation of gene expression (Jarmoskaite and Russell, 2014; Tanner and Linder, 2001; Jankowsky, 2011). They also play an important role in sensing viral RNAs in the context of the innate immune system (Schlee *et al*., 2009). RNA helicases outnumber DNA helicases and they often perform functions substantially different from

those attributed to DNA helicases. However, in terms of structure and sequence, RNA helicases are closely related to DNA helicases (Fairman-Williams *et al*., 2010).

1.2 The Mechanism of Helicases

A complete understanding of the mechanism of nucleic acid unwinding and/or translocation by a motor protein requires information regarding the oligomeric structure of the functional enzyme, as well as the translocation mechanism, directional bias, step size, rate and ATP hydrolysis.

During genome replication, repair, and recombination, helicases need to unwind nucleic acids much longer than their binding sites, so the helicase stays on track and catalyzes repeated cycles of base pair separation steps. Base pair separation takes place at single-stranded/double-stranded junction regions. Helicases unwind long stretches of duplex nucleic acids by coupling base pair separation to translocation. In general, mechanisms of helicase-catalyzed DNA or RNA unwinding can be classified as either "active" or "passive" (Amaratunga and Lohman, 1993; Lohman and Bjornson, 1996; Manosas *et al*., 2010; von Hippel and Delagoutte, 2001).

In a passive mechanism, the helicase does not interact with the double strand DNA (dsDNA). Instead it uses its directional single-stranded DNA (ssDNA)-translocase activity to move onto and thus stabilize ssDNA, which has resulted from transient base-pair opening and closing fluctuations. Many ring-shaped (T7 gp4, DnaB, MCM) and non-ring-shaped helicases (NPH II, Dda) have been proposed to unwind nucleic acid by this mechanism (Jezewska *et al*., 1998; Kaplan, 2000; Kaplan *et al*., 2003; Kawaoka *et al*., 2004; Tackett *et al*., 2001). This mechanism and the mode of nucleic acid binding provide a way to prevent immediate reannealing of the unwound strands (Velankar *et al*., 1999).

In the active mechanism, the helicase interacts directly with the double-strand near the unwinding junction region and distorts it prior to fully separating the strands by directional translocation (Velankar *et al*., 1999; Wong and Lohman, 1992). Such a mechanism has

been proposed for the PcrA helicase based on a crystal structure that showed interactions of the 2B domain with the duplex DNA (Cheng *et al*., 2002). In active mechanisms, the stepping models have generally been described as inch-worm mechanisms for monomeric translocases, which require the translocase to have at least two nucleic acid binding sites (Velankar *et al*., 1999; Yarranton and Gefter, 1979; Yu *et al*., 2006; Hill and Tsuchiya, 1981; Soultanas and Wigley, 2001). In the inchworm mechanisms, the two binding sites bind and release nucleic acid in response to the signals received from the NTPase site (Wong and Lohman, 1992; Velankar *et al*., 1999; Yarranton and Gefter, 1979). A cycle of nucleic acid binding, release, and translocation events begins with one helicase site bound tightly to the nucleic acid and the second helicase site bound weakly to the nucleic acid (**Fig. 1.1A**). Rolling or hand-over-hand mechanisms applicable to multisubunit helicases have also been proposed (Wong and Lohman, 1992), although the evidence that led to the proposal of the rolling model is also consistent with a "dimeric inch-worm model". If there is only one possible nucleic acid binding site, the helicase may move unidirectionally along the nucleic acid using a Brownian motor or ratchet type mechanism (Levin *et al*., 2005; Astumian, 1997). In the weak state, the helicase can move in either direction (Brownian motion) along the nucleic acid. When the helicase resumes the tight state, it makes a step forward (power stroke). Those molecules that have fluctuated in the forward direction move ahead and those that have fluctuated in the opposite direction return to the original position. Repetition of these steps leads to net forward movement of the helicase along the nucleic acid (**Fig. 1.1B**).

Even though the helicase core domains share a similar three-dimensional fold and many helicase family members display helicase activities as monomers, they often assemble into various oligomeric states or work as part of a larger protein complex to display full activity. The hexamer is the most established oligomerization state in which six subunits assemble to form a ring-shaped structure (e.g., T7 gp4, *E. coli* DnaB, RepA, Rho, MCM, and SV40-LTag) (Patel and Picha, 2000). However, the single subunit of these ring-shaped

helicases (T7 gp4) is not active in catalyzing nucleotide hydrolysis or unwinding reactions, suggesting hexamer formation is essential for their function (Guo *et al.*, 1999). Moreover, the ring-shaped structure is stabilized by the binding of NTP, a divalent metal ion, or both, and by the nucleic acid substrate (Patel and Picha, 2000). The enclosure of the nucleic acid by the protein subunits decreases the probability of the helicase falling off, thus increasing the ability of the helicase to maintain processivity. Another advantage of this arrangement is that the coupling of NTPase cycles between the hexameric subunits can increase the efficiency of promoting translocation. Oligomerization is also an important strategy for non-ring-shaped helicases as well, and they have mainly been considered to be

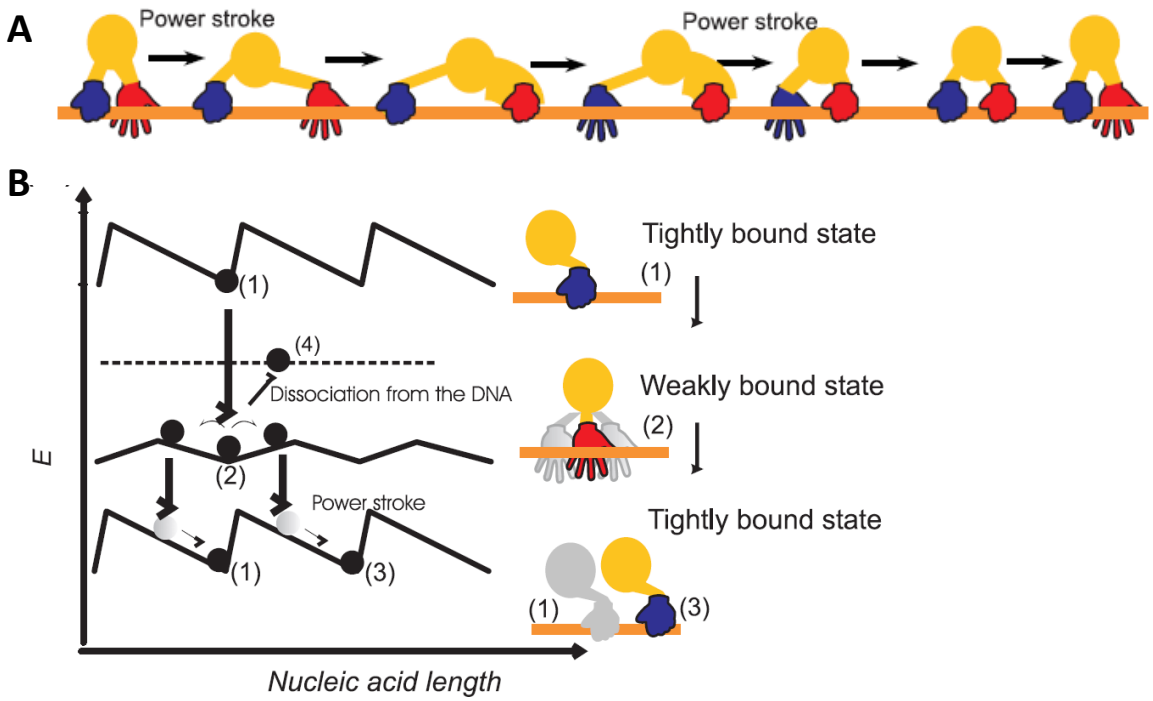

Fig. 1.1 Proposed mechanisms of translocation and strand separation of helicase. Stepping inchworm mechanism. A helicase monomer with a tight (closed hand) and a weak (open hand) nucleic acid binding site is shown to undergo steps of helicase movement (power stroke) and nucleic acid affinity changes. (**B**) Brownian motor mechanism. On the right, the helicase is shown to undergo nucleic acid affinity changes (tight to weak). In the weak state (2), the helicase fluctuates in either direction. Upon resuming the tight state (3), some helicase molecules move forward (3) and some return to their original position (1). On the left, the free energy of the helicase-nucleic acid complex is shown along the nucleic acid length. (Patel and Donmez, 2006. Reprinted with permission)

monomeric or dimeric (Patel and Donmez, 2006). Most non-ring shaped helicases function as monomers (e.g., T4 phage Dda, HCV NS3h, and *E. coli* RecQ) (Nanduri *et al*., 2002; Xu *et al*., 2003; Levin *et al*., 2004) and their activity is greatly enhanced by the formation of dimers or higher oligomers (Maluf *et al*., 2003; Cheng *et al*., 2001; Byrd and Raney, 2005; Levin *et al*., 2004).

1.3 Superfamily 2 Helicases

Based on the presence and the structure of helicase motifs along with their functional analysis, helicases have been classified into six superfamilies (SF) (Singleton *et al*., 2007). Helicases of different families share similarities in their three-dimensional folds, with two RecA-like domains making up the helicase core (Subramanya *et al*., 1996; Bird *et al*., 1998; Singleton *et al*., 2000). SF1 and SF2 helicases are closely related and typically contain several domains and a single NTP binding site at the interface of the two RecA-like domains. RecA is a 38 kDa protein essential for the repair and maintenance of DNA. SF1 and SF2 helicases can function as monomers, dimers or larger oligomers (Mackintosh and Raney, 2006). Besides SF1 and SF2, the other helicases are classified into four families: SF3 (e.g., papilloma virus E1), SF4 (e.g., DnaB-like), SF5 (e.g., Rho/V-F-ATPases), and SF6 (e.g., AAA^{+}-like family). Most SF3-6 helicases are hexameric (or double-hexameric) rings formed from 6 (or 12) individual RecA folds.

Helicase superfamily 2 is the largest and most diverse of the helicase superfamilies (Byrd and Raney, 2012). They are RNA-dependent ATPases and ATP-dependent RNA binding proteins and a few have activity with DNA substrates as well (Hilbert *et al*., 2009). It has been further divided into sub-families including RecQ-like, RecG-like, Rad3/XPD, Ski2-like, type I restriction enzyme, RIG-I-like, NS3/NPH-II, DEAH/RHA, DEAD-box, and Swi/Snf families based on sequence homology (Fairman-Williams *et al*., 2010; Jankowsky and Bowers, 2006; Jankowsky and Fairman, 2007). One of the most notable SF2 helicase signatures are the characteristic sequence motifs (**Fig. 1.2A**). The conversion

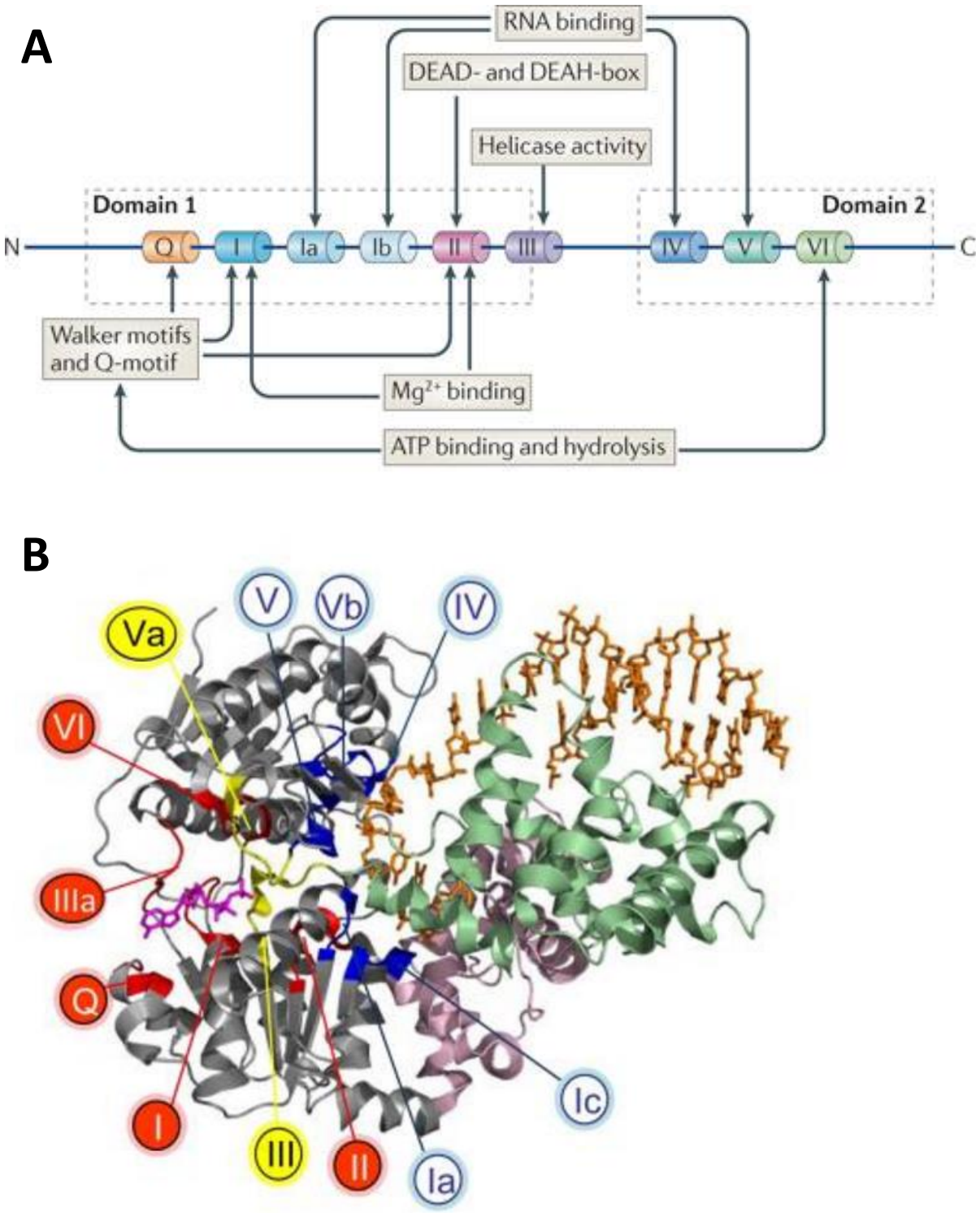

Fig. 1.2 Conserved motifs in superfamily 2 helicases. (**A**) Sequence organization of the helicase core motifs in SF2 (Parsyan *et al*., 2011. Reprinted with permission). (**B**) Position of the characteristic motifs in three-dimensional structures of SF2 proteins. The bound ATP analog is colored margenta, the nucleic acid is colored wheat. (From Fairman-Williams *et al*., 2010. Reprinted with permission).

of energy derived from NTP hydrolysis into unwinding of double-stranded nucleic acids is coordinated by 9 sequence motifs (Q, I, Ia, Ib, II, III, IV, V and VI) (Singleton *et al*., 2007). Of these 9 motifs, 7 motifs are most conserved during evolution, and are usually clustered in a region of 200 – 700 amino acids called the helicase core domain. Generally, motifs I, II, and VI are essential for ATP binding and hydrolysis, motifs Ia, IV and V are primarily responsible for DNA binding, and motif III is important for coupling ATP hydrolysis to remodeling events such as unwinding. The highest level of sequence conservation across SF2 is seen in the residues that coordinate binding and hydrolysis of the triphosphate (motifs I, II, and VI). These residues are located in the cleft between the two conserved RecA-like helicase domains (**Fig. 1.2B**).

The spatial arrangement of functionalities presented by these residues is highly conserved in other P-loop NTPases (Phosphate-binding loop, a conserved sequence motif in proteins that is associated with phosphate binding with pattern Gly-X4-Gly-Lys-(Thr/Ser)), probably reflecting significant evolutionary constraints in the active site for phosphoester hydrolysis (Leipe *et al*., 2002). Most well-characterized SF2 members display 3′→5′ polarity. Exceptions include the Rad3/XPD family members, which are characterized by the presence of an iron-sulfur cluster in the N-core domain (Rudolf *et al*., 2006) (discussed in the next section).

SF2 helicases are involved in transcription, DNA repair, and chromatin remodeling (Bennett and Keck, 2004; Fuller-Pace, 2006; Lusser and Kadonaga, 2003) and all aspects of RNA metabolism (Pyle, 2008). Since SF2 helicases function in many parts of nucleic acid metabolism, defects of these helicases are associated with a variety of diseases including predisposition to cancer, premature aging, immunodeficiency, and mental retardation (van Brabant *et al*., 2000; Ellis, 1997). For example, mutations in human XPB helicase cause defects in both transcription and DNA repair, leading to at least three severe genetic disorders: xeroderma pigmentosum, cockayne syndrome and trichothiodystrophy (Giglia-Mari *et al*., 2004; Lehmann, 2003); defects in BLM helicase cause Bloom syndrome

which is associated with a very high incidence of different types of cancers, both solid tumors and leukemia (Ellis *et al*., 1995); RECQ4 mutations are associated with an autosomal recessive disorder RAPADILINO syndrome (Siitonen *et al*., 2003). Dysfunction of RNA helicases, such as eIF4A mutations, also cause diseases and lead to melanoma, liver, lung, colon and breast cancer (Svitkin *et al*., 2001). Finally, alter DDX1 expression in human astrocytes is responsible for the unfavorable cellular microenvironment for HIV-1 infection (Fang *et al*., 2005; Robertson-Anderson *et al*., 2011).

1.4 Rad3/XPD Family

Rad3 helicase is encoded by the *RAD3* gene of *Saccharomyces cerevisiae*, and it is required for cell viability and excision repair of damaged DNA (Guzder *et al*., 1994). Rad3 is also involved in the maintenance of the fidelity of DNA replication and acts as a component of the general transcription factor IIH (TFIIH) core (Sung *et al*., 1996). The ortholog of Rad3 in humans is XPD, Xeroderma pigmentosum complementation group D protein. Because the Rad3/XPD family helicases contain a conserved iron-sulfur cluster via four cysteine residues, they are commonly referred to as Fe-S helicases. Rad3/XPD family members are critical for many aspects of genome maintenance. XPD is a part of the transcription factor TFIIH that is involved in nucleotide excision repair as well as in transcription initiation. Four human XPD paralogs (XPD, FANCJ, RTEL1 and ChlR1) are DNA helicases with roles in DNA repair and genome maintenance (Wu *et al*., 2009; Wu and Brosh, Jr., 2012) (**Fig. 1.3 A**). All of these helicases are implicated in autosomal recessive genetic diseases: ChlR1 in Warsaw Breakage Syndrome (van der Lelij *et al*., 2010); FANCJ in Fanconi anemia and breast cancer (Cantor *et al*., 2001; Levitus *et al*., 2005; Litman *et al*., 2005; Levran *et al*., 2005); XPD in xeroderma pigmentosum, cockayne syndrome, trichothiodystrophy, and cerebro-oculo-facio-skeletal syndrome (DiGiovanna and Kraemer, 2012); and RTEL1 in Hoyeraal–Hreidarsson syndrome, dyskeratosis congenita (Ballew *et al*., 2013; Le *et al*., 2013). Members of the Rad3/XPD-like helicase family play distinct

and only partially overlapping roles in the cell (**Fig 1.3 A**). However, all of them are likely to share the overall structure and basic mechanism of DNA translocation and unwinding.

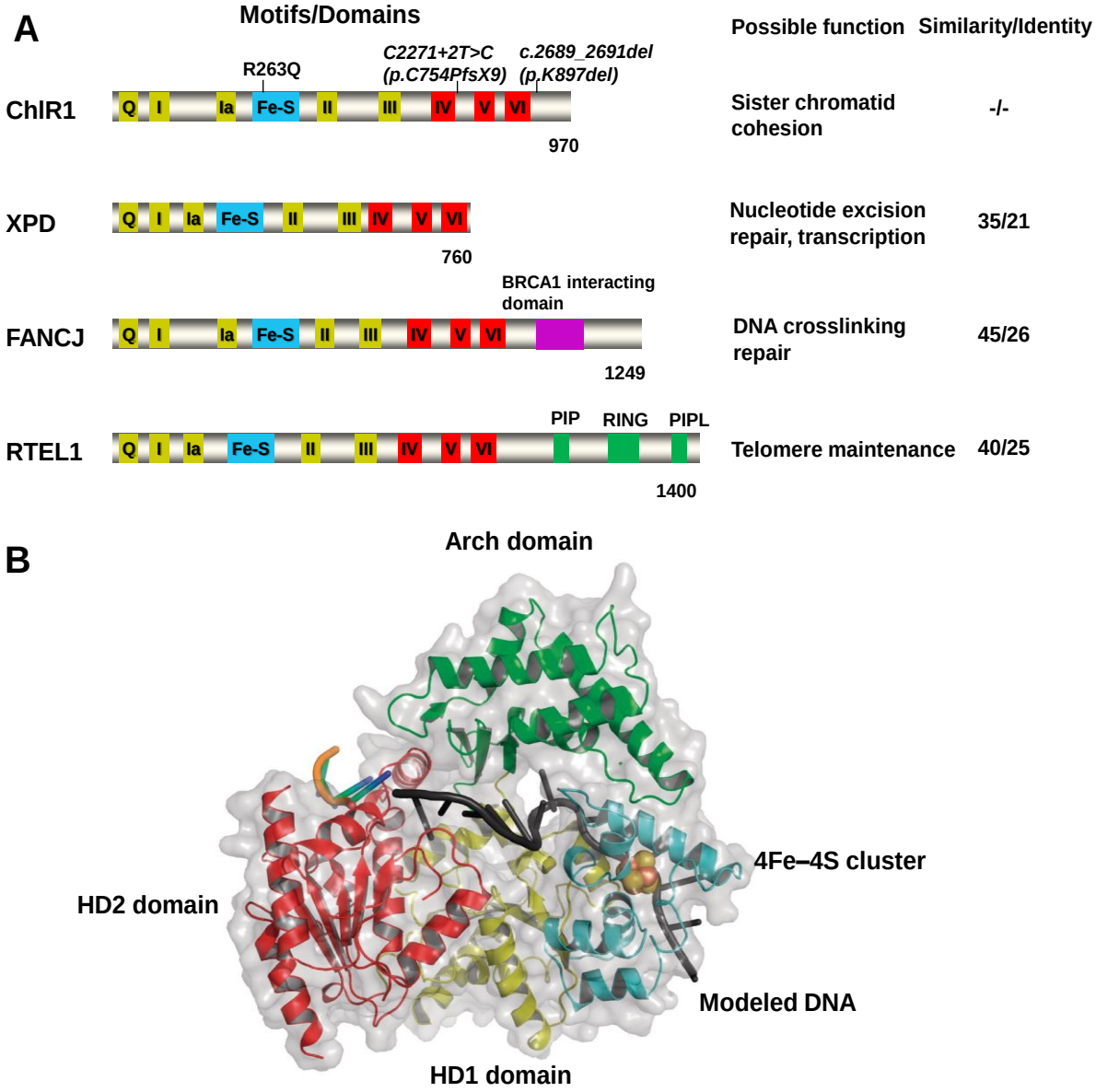

Fig. 1.3 Helicase core motifs and the structure of TaXPD. (**A**) Members of Rad3/XPD DNA helicases family. They contain a conserved ATPase/helicase core domain characterized by the eight conserved helicase motifs (HD1 domaim in yellow, HD2 domain in red) and Fe–S cluster domain (Blue). (**B**) Overall structure of TaXPD (PDB # 4A15) with the two RecA-like domains (HD1 and HD2 domains) in yellow and red, the Fe-S cluster domain in blue, and the arch domain in green. The 4Fe–4S cluster is shown by the spheres with orange (Fe atom) and yellow (Cys residue) colors. Combination of experimentally verified DNA is shown in orange with modeled DNA shown in gray (From Kuper *et al.*, 2012. Reprinted with permission).

Rad3/XPD helicases are comprised of four domains, RecA-like HD1, RecA-like HD2, 4Fe-S, and Arch (Rudolf *et al*., 2006) (**Fig. 1.3 B**). All characterized XPD-like helicases move along ssDNA in a 5'→3' direction (Pugh *et al.,* 2008; Rudolf *et al.,* 2006; Voloshin *et al*., 2003). Current structural information on Fe-S helicases is limited to three apo structures of archaeal XPD homologs (Fan *et al*., 2008; Liu *et al*., 2008; Wolski *et al*., 2008) and a taXPD structure in a complex with a 5 nucleotide ssDNA fragment bound to the HD2 outside of the classical DNA binding site (Kuper *et al*., 2012). Recently, a truncated XPD structure was solved (PDB# 5H8C), which may provide more information on the exact strunctures and functions for other Rad3/XPD family members. The Fe-S cluster has dual functions to stabilize elements of protein secondary structure and to target the helicase to the single-stranded/double-stranded DNA junction (Pugh *et al*., 2008). Human FANCJ, RTEL1, and ChlR1 are likely to share the basic molecular mechanism of DNA translocation and unwinding, as well as a common arrangement of helicase core motifs.

1.5 ChlR1 Helicase (DDX11)

ChlR1, also known as DDX11, is a superfamily 2 DNA helicase that contains a conserved iron-sulfur domain (**Fig 1.4**). The functions of ChlR1 appear to be conserved throughout evolution. A role of the ChlR1 helicase in sister chromatid cohesion was evidenced by studies of the ChlR1 homolog in yeast and human. Yeast Chl1 binds to components of the replication machinery, implicating a role of Chl1p to preserve genomic stability by promoting proper chromosome segregation and efficient sister chromatid cohesion during the S phase (Mayer *et al*., 2004; Rudra and Skibbens, 2013; Skibbens, 2004; Tsay *et al*., 2009).

RNAi-dependent down regulation of human ChlR1 causes premature sister chromatid separation and a profound delay in mitotic progression in human cells, suggesting that ChlR1 is required to establish proper sister chromatid cohesion during S-phase (Parish *et al*., 2006). Subsequent RNA interference studies with human cells showed that ChlR1 is

required for proper chromosome cohesion at both the centromeres and along the chromosome arms, as well as tight binding of cohesion complexes to chromatin (Inoue *et al.*, 2007; Shah *et al.*, 2013). Loss of ChlR1 in the mouse resulted in embryonic lethality, which suggests that the aneuploidy apparent in *Ddx11*$^{-/-}$ embryos was a consequence of sister chromatid cohesion defects and placental malformation (Inoue *et al.*, 2007)

Mutations in human ChlR1 are genetically linked to Warsaw Breakage Syndrome (WABS), which is characterized by severe microcephaly, pre- and postnatal growth retardation, and abnormal skin pigmentation (van der Lelij *et al.*, 2010). A patient diagnosed with WABS carried compound heterozygous mutations in ChlR1, a splice site mutation and a 3-bp in-frame C-terminal deletion (c.2689_2691del [p.K897del]) that was shown to abrogate the ChlR1 helicase activity (Wu *et al.*, 2012a). Cells from the patient exhibited chromosomal instability characterized by sister chromatid cohesion defects,

```
                          Q                                I
MANETQKVGAIHFPFPFTPYSIQEDFMAELYRVLEAGKIGIFESPTGTGKSLSLICGALSWLRDFEQKKR

EEEARLLETGTGPLHDEKDESLCLSSSCEGAAGTPRPAGEPAWVTQFVQKKEERDLVDRLKAEQARRKQR

EERLQQLQHRVQLKYAAKRLRQEEEERENLLRLSREMLETGPEAERLEQLESGEEELVLAEYESDEEKKV
                       Ia
ASRVDEDEDDLEEEHITKIYYCSRTHSQLAQFVHEVKKSPFGKDVRLVSLGSRQNLCVNEDVKSLGSVQL

INDRCVDMQRSRHEKKKGAEEEKPKRRRQEKQAACPFYNHEQMGLLRDEALAEVKDMEQLLALGKEARAC
                                    II
PYYGSRLAIPAAQLVVLPYQMLLHAATRQAAGIRLQDQVVIIDEAHNLIDTITGMHSVEVSGSQLCQAHS

QLLQYVERYGKRLKAKNLMYLKQILYLLEKFVAVLGGNIKQNPNTQSLSQTGTELKTINDFLFQSQIDNI

NLFKVQRYCEKSMISRKLFGFTERYGAVFSSREQPKLAGFQQFLQSLQPRTTEALAAPADESQASTLRPA
                                                        III
SPLMHIQGFLAALTTANQDGRVILSRQGSLSQSTLKFLLLNPAVHFAQVVKECRAVVIAGGTMQPVSDFR

QQLLACAGVEAERVVEFSCGHVIPPDNILPLVICSGISNQPLEFTFQKRELPQMMDEVGRILCNLCGVVP
        IV                                                              V
GGVVCFFPSYEYLRQVHAHWEKGGLLGRLAARKKIFQEPKSAHQVEQVLLAYSRCIQACGQERGQVTGAL
                                                                   VI
LLSVVGGKMSEGINFSDNLGRCVVMVGMPFPNIRSAELQEKMAYLDQTLPRAPGQAPPGKALVENLCMKA

VNQSIGRAIRHQKDFASVVLLDQRYARPPVLAKLPAWIRARVEVKATFGPAIAAVQKFHREKSASS-906
```

Fig. 1.4 Human ChlR1 amino acid sequence. Seven helicase motifs indicated with yellow and Q motif with blue. The signature motif II sequence (DEAH) is in bold. The patient mutations R263Q and K897del are indicated in red, the possible trypsin cleavage sites are indicated in green (Predicted by DNASTAR-Lasergene Protean 3D).

chromosomal breakage, and sensitivity to the DNA cross-linking agent, mitomycin C and the topoisomerase inhibitor, camptothecin (van der Lelij *et al*., 2010). In a second reported WABS case, three affected siblings who carry a homozygous missense mutation (R263Q) in the conserved Fe-S domain showed severe intellectual disability and many of the congenital abnormalities reported in the original case. The biochemical assays revealed the point mutation impaired helicase activity by perturbing its DNA binding and DNA-dependent ATP hydrolysis (Capo-Chichi *et al*., 2013). Recently, a third case was reported that shares similar phenotypic features to the previously reported cases, including pre- and postnatal growth retardation, severe microcephaly, intellectual disability, facial dysmorphism and hearing loss due to cochlea abnormalities (Bailey *et al*., 2015).

ChlR1 has been shown to interact preferentially with forked duplex DNA, and efficiently unwinds the 5' flap structure, a key intermediate of lagging strand processing (Wu *et al*., 2012a). Also, ChlR1 can interact with Fen1 (Flap endonuclease 1) and stimulate its 5' flap endonuclease activity (Farina *et al*., 2008). Chl1 promotes Scc2 (component of cohesion complex) loading unto DNA such that both Scc2 and cohesion enrichment to chromatin are defective in Chl1 mutant cells (Rudra and Skibbens, 2013). Both Chl1 expression and chromatin-recruitment are tightly regulated throughout the cell cycle, peaking during S-phase.

Biochemically, the purified recombinant ChlR1 protein showed that it is a DNA-dependent ATPase and unwinds partial duplex DNA substrates with a preferred 5' to 3' polarity during DNA-replication (Hirota and Lahti, 2000; Farina *et al*., 2008). ChlR1 interacts with Ctf18-RFC, PCNA, and FEN-1 and stimulates FEN-1 endonuclease activity on an equilibrating flap DNA structure, a model intermediate substrate that forms during lagging strand synthesis (Farina *et al*., 2008). ChlR1 unwinds G-quadruplex (G4) DNA with a strong preference for a two-stranded antiparallel G4 (G2') substrate and is only marginally active on a four-stranded parallel G4 structure (Wu *et al*., 2012a). It was proposed that ChlR1 involvement in lagging strand processing during cellular DNA

replication may be important for sister chromatid cohesion (Rudra and Skibbens, 2012). Recently it was shown in yeast that Chl1 promotes the loading of Scc2, a cohesion regulatory factor, on to chromatin specifically during the S phase (Rudra and Skibbens, 2013). The Timeless-Tipin protein complex that is implicated in replication fork stabilization and sister chromatid cohesion interacts with ChlR1 (Leman *et al*., 2010), supporting the notion that the DNA helicase collaborates with other factors to maintain a fork structure conducive to establishment of cohesion. However, the precise molecular pathways whereby ChlR1 maintains genomic stability are not well understood.

1.6 The Q motif in Helicases

The Q motif (Gly-Phe-X-X-Pro-X-Pro-Ile-Gln) was first identified in DEAD box RNA helicases a decade ago (Tanner *et al*., 2003). It is located 17 amino acids upstream of motif I and consists of a nine amino acid sequence containing an invariant glutamine (Q) residue (**Fig. 1.5**). Compared with the conserved seven helicase motifs, the Q motif is somewhat less conserved among SF2 helicases. Site-specific mutagenesis studies demonstrate that the Q motif controls ATP binding and hydrolysis in the yeast translation-initiation factor RNA helicase eIF4A, and *in vivo* analyses in yeast showed that the Q motif and upstream aromatic group are important for cell viability (Tanner *et al*., 2003). The Q motif was also shown to be important for ATPase activity of a viral helicase, NS3 (Gallivan and McGarvey, 2003).

Several helicase structural studies demonstrated that the Q motif glutamine side chain hydrogen binds to the Adenine base, providing specificity for binding ATP (**Fig. 1.6**) (Del and Lambowitz, 2009; Lee and Yang, 2006; Newman *et al*., 2015). For example, the Q motif of Bloom's syndrome helicases (RecQ family member) is crucial for conferring nucleotide triphosphate specificity. The adenine base of the ADP lies between the side chains of L665 and R669, and makes a bivalent hydrogen bond to Q672 (**Fig. 1.6**). These residues are part of the Q motif in Bloom's syndrome helicases. (Newman *et al*., 2015)

Another recent paper solved the structure of *C. sakazakii* RecQ helicase and demonstrated that the Glutamine in the Q motif is also responsible for binding the adenine in ATP (Manthei *et al.*, 2015). The Q motif regulates not only ATP binding and hydrolysis but also the affinity of yeast RNA helicase Ded1 for RNA substrates and its helicase activity (Cordin *et al*., 2004). Mutagenesis studies in the Q motif in RNA helicases concluded that it directly regulates the affinity of the protein for the substrate (RNA) through conformational changes associated with nucleotide binding (Worrall *et al*., 2008; Cordin *et al*., 2004). It was further proposed that the Q motif in eIF4A and Ded1 RNA helicases functions as a molecular on-off switch for ATP hydrolysis and helicase activity (Tanner, 2003). The effect of glutamic acid substituted for the invariant glutamine within the Q

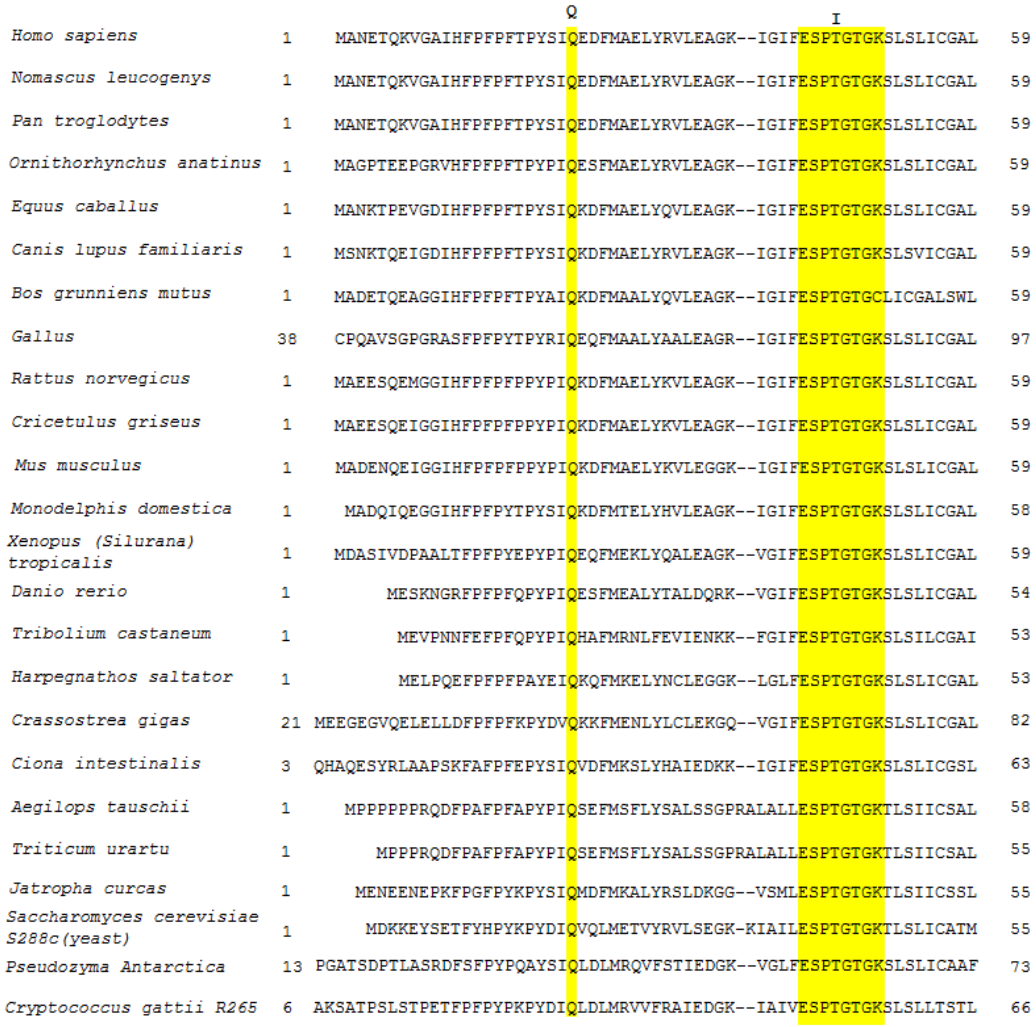

Fig. 1.5 Sequence alignment of ChlR1 helicase across species. The helicase motif Q and motif I are marked with yellow.

motif was studied in the RNA helicase Hera. This work suggested that the Q motif is responsible for sensing the nucleotide state of the helicase and establishing a stable interaction of the Walker A box (P-loop) with other helicase motifs, and this stabilization is required for catalytic competence (Strohmeier *et al*., 2011).

Several crystal structures of DNA helicases have been studied showing that the conserved glutamine is structurally important for nucleotide binding. The crystal structures of the ATP-bound *Escherichia coli* UvrB (Theis *et al*., 1999), PcrA (Velankar *et al*., 1999), RecQ (Bernstein *et al*., 2003), and UvrD (Lee and Yang, 2006) helicases show the conserved glutamine of the Q motif forms a bidentate hydrogen bond with the adenine base; however, its precise role(s) in the biochemical functions of DNA helicases is less well understood. For example, the Q motif of the phage λ packaging motor was shown to be involved in DNA-motor interactions and governs its force-generating ability (Tsay *et al*., 2009). However, a recent study of SWI2/SNF2 domain-containing protein ADAAD (a fragment of SMARCAL1) suggests that the Q motif is required for ATP hydrolysis but not ATP binding (Nongkhlaw *et al*., 2012). Another study demonstrated that the Q motif of FANCJ helicase regulates its dimerization and DNA binding (Wu *et al*., 2012b). Thus, the role of the Q motif in helicases is inconclusive.

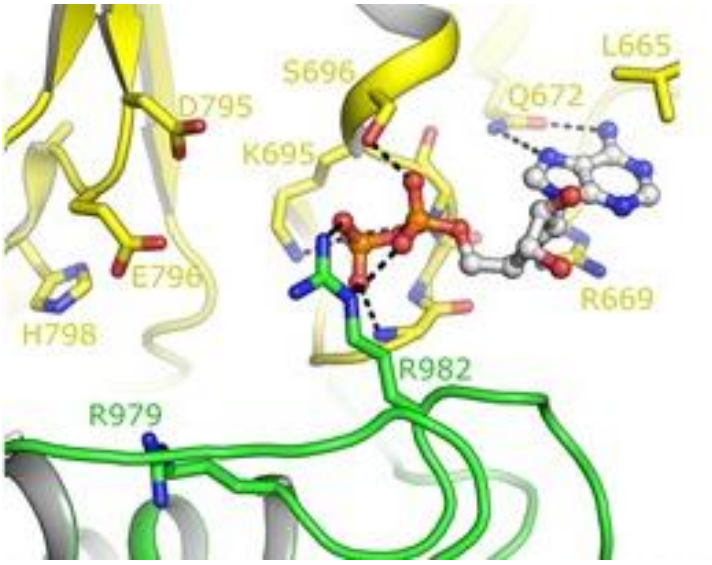

Fig. 1.6 The coordination of ADP and helicase motifs in Bloom's syndrome helicase helicase. The adenine base is s specifically selected by Q672 (Q motif) through bifurcated hydrogen bonds. (From Newman *et al*., 2015. Reprinted with permission)

2. Hypothesis and Objectives

2.1 Hypothesis

We hypothesize that the Q motif in ChlR1 helicase is important for its helicase activity, thus the Q motif may affect ChlR1's cellular functions.

2.2 Objectives:

1) To characterize the catalytic activities of the ChlR1 Q motif mutant of. I will examine the proteins' enzymatic activities, including ATP binding and hydrolysis, DNA binding, protein displacement, and helicase activity;

2) To determine the role of the Q motif in the oligomerization state of ChlR1 protein;

3) To detect the structure differences between ChlR1-WT protein and the Q motif mutant protein;

4) To examine the cellular function of the Q motif in ChlR1 helicase.

3. Experimental Procedures

3.1 Plasmid DNA and Mutagenesis

The human *ChlR1* cDNA was subjected to PCR amplification using primers ChlR1-F-*Hind*III and ChlR1-R-*Xho*I (**Table 1**). The PCR product, which includes a 3× FLAG tag at the C-terminus, was cloned into the *Hind*III and *Xho*I sites of pcDNA3 (Invitrogen). The Q23A and K50R mutations were generated by a QuikChange site-directed mutagenesis kit (Stratagene) according to the manufacturer's instructions using the designed mutagenic primers shown in **Table 1**. For bacterial overexpression, the human *ChlR1* gene was cloned into the *Nde*I and *Xho*I sites of pET28a vector (Novagen). All plasmids were sequenced to verify that no undesired mutations were introduced during PCR and cloning. The reagents, names, and addresses of suppliers that were used in the experiments are listed in **Table 2**.

3.2 DNA Substrates

PAGE-purified oligonucleotides used for the preparation of DNA substrates, DC26 and $T_{STEM}25$, were purchased from IDT (**Table 1**). The duplex, triplex and G-quadruplex substrates were 5' ^{32}P-end-labeled and prepared as described previously (Wu *et al*., 2008). For the triplex DNA substrate, the plasmid pSupF5 contains a duplex sequence that serves as a target for TC30 (Brosh, Jr. *et al*., 2001). Cleavage of the plasmid with *Nde*I released fragments of 4 and 0.6 kb. The triplex site lies 1800 bases from one end of the large fragment. Triplexes were prepared by incubation of 3 pmol of ^{32}P-labeled TC30 oligonucleotide (**Table 1**) overnight at room temperature with 6 pmol of *Nde*I-cleaved plasmid in a buffer containing 33 mM Tris acetate (pH 5.5), 66 mM KOAc, 100 mM NaCl, 10 mM MgCl2, and 0.1 mM spermine. The complexes were then separated from unbound oligonucleotide by SEC using Bio-Gel A-5M resin (Bio-Rad). The 30-mer flush triplex substrates were prepared by incubation of the TC30 oligonucleotide with the previously annealed 30-bp duplex (TC30W and TC30C) under the annealing conditions.

Table 1 DNA oligomers used in this study

Oligonucleotide/ DNA substrate	Structure and sequence (5'-3')	Used in this study
ChlR1-Q23A-F	CACACCCTATTCCATCGCGGAAGACTTCATGGCAG	Forward primer for Q23A mutagenesis
ChlR1-Q23A-R	CTGCCATGAAGTCTTCCGCGATGGAATAGGGTGTG	Reverse primer for Q23A mutagenesis
ChlR1-K50R-F	CCAACTGGCACTGGGAGGTCCTTAAGTCTTATTTG	Forward primer for K50R mutagenesis
ChlR1-K50R-R	CAAATAAGACTTAAGGACCTCCCAGTGCCAGTTGG	Reverse primer for K50R mutagenesis
Forked duplex	 DC26: TTTTTTTTTTTTTTTTTTTTTCCCAGTAAAACGACGGCCAGTGC $T_{STEM}25$: GCGGTCCCAAAAGGGTCAGTGCTGGCATTTTGCTGCCGGTCACG	DC26 was either ^{32}P or fluorescence labeled, and used as dsDNA substrate
OX-1 G2'	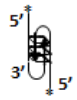 OX-1: ACTGTCGTACTTGATATTTTGGGGTTTTGGGG	A two-stranded antiparallel G4 (G2') substrate
TP-G4	 TP: TGGACCAGACCTAGCAGCTAGGGGGAGCTGGGGAAGGTGGGAATGTGA	A four-stranded parallel G4 (G4') substrate
5' Tail flush triplex	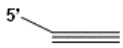 5'Tail TC30: TGACGCTCCGTACGATCTTTTTCTTTCTTT TCTTCTTTTTTCTTT. TC30W: TTTCTTTTTTCTTCTTT TCTTTCTTTTTCT; TC30C: AGAAAAAGAAAGAAAAG AAGAAAAAAGAAA. TC30W and TC30C are used to form duplex DNA, and 5' tail TC30 as third strand	A short triplex DNA substrate
5'Tail plasmid triplex	 Plasmid pSupF5 is linearized by digestion with NdeI, and the third strand is annealed to triplex target site in duplex. 5' tail TC30 is used as third strand.	A long triplex DNA substrate

Table 2 List of Reagents and Suppliers

Reagents	Suppliers	Address
2-log DNA ladder, N3200L	Biolab	Lawrenceville, Georgia, USA
Acrylamide, 0314	AMRESCO	North York, Ontario, Canada
Adenosine Triphosphate (ATP), A1852	Sigma-Aldrich	Oakville, Ontario, Canada
Adenosine Diphosphate (ADP), A2754	Sigma-Aldrich	Oakville, Ontario, Canada
Adenylyl-imidodiphosphate (AMP-PNP), A2647	Sigma-Aldrich	Oakville, Ontario, Canada
Agarose, 5510UB	Gibco	Burlington, Ontario, Canada
Ampicillin, A1593	Sigma-Aldrich	Oakville, Ontario, Canada
Ammonium persulfate (APS), A3678	Sigma-Aldrich	Oakville, Ontario, Canada
Boric Acid, SLBC5554V	Sigma-Aldrich	Oakville, Ontario, Canada
Bradford protein assay reagent, 500-0013	Bio-Rad	Hercules, California, USA

Table 2 Continued

Reagents	Suppliers	Address
dNTPs, N0447S	NEB	Mississauga, Ontario, Canada
Dulbecco's Modified Eagle Medium (DMEM), SH30022.01	Sigma-Aldrich	Oakville, Ontario, Canada
Yeast Extract, J850	AMRESCO	North York, Ontario, Canada
Fetal Bovine Serum (FBS), F6178	Sigma-Aldrich	Oakville, Ontario, Canada
Glycine, BP381-5	Fisher Scientific	Madison, Wisconsin, USA
Glycerol, 123170	Fisher Scientific	Madison, Wisconsin, USA
Kanamycin, 60615	Sigma-Aldrich	Oakville, Ontario, Canada
Lysogeny Broth (LB) with agar, L2897	Sigma-Aldrich	Oakville, Ontario, Canada
Methanol, 154246	Fisher Scientific	Madison, Wisconsin, USA
Non-fat dry milk, 170-6404	Bio-Rad	Hercules, California, USA
Nonidet P-40, 74385	Sigma-Aldrich	Oakville, Ontario, Canada
N,N,N',N'-Tetramethylethylenediamine (TEMED), 87689	Sigma-Aldrich	Oakville, Ontario, Canada
Penicillin-Streptomycin, 084M4778V	Sigma-Aldrich	Oakville, Ontario, Canada
Phenylmethylsulfonyl fluoride (PMSF), P7626	Sigma-Aldrich	Oakville, Ontario, Canada
Protein standard, 161-0374	Bio-Rad	Hercules, California, USA
Protease inhibitor, 05892791001	Roche	Mannheim, Germany
Sodium dodecyl sulfate (SDS), L3771	Sigma-Aldrich	Oakville, Ontario, Canada
Sodium chloride (NaCl), S671-10	Fisher Scientific	Madison, Wisconsin, USA
T4 DNA LIGASE, M0202S	Biolab	Lawrenceville, Georgia, USA
Q5® Hot Start High-Fidelity DNA Polymerase, M0493S	NEB	Mississauga, Ontario, Canada
Tris, 0826	AMRESCO	North York, Ontario, Canada
Triton™ X-100, X100	Sigma-Aldrich	Oakville, Ontario, Canada
Trypsin-EDTA, T4049	Sigma-Aldrich	Oakville, Ontario, Canada
Trypsin, 85450C	Sigma-Aldrich	Oakville, Ontario, Canada
Tryptone, TRP402.205	Bioshop	Burlington, Ontario, Canada
TWEEN® 20, BP337	Fisher Scientific	Madison, Wisconsin, USA
Western Blotting detection reagent, RPN2232	GE Health Care	Little Chalfont, UK

3.3 The Expression and Purification of ChlR1 Recombinant Protein

The PEI transfection system (Boussif *et al*., 1995) was used to transfect ChlR1 plasmid DNA into HEK293T cells, which were maintained in complete DMEM (Cat# 12-604F, Lonza) containing 10% fetal bovine serum (Cat# F1051, Sigma) and 50 μg/ml penicillin streptomycin (Cat# P4333, Sigma). The recombinant ChlR1 proteins were purified with a protocol described by Wu *et al*., (2012a) with modifications. Briefly, cell pellets were resuspended in buffer A (10 mM Tris HCl (pH 7.4), 10 mM KCl, 1.5 mM $MgCl_2$, 1 mM DTT, 0.5 mM PMSF, protease inhibitors). Cell suspension was lysised by sonication in the presence of protease inhibitors (Roche Applied Science) at 4°C, 10 short burst of 10 sec followed by intervals of 30 sec for cooling. The lysised cells were centrifuged at 43,500 g for 30 min at 4°C. The supernatant was incubated with FLAG antibody resin (Cat# F2426, Sigma) for 2 h at 4°C. The resin was washed twice with buffer B (20 mM Tris HCl (pH 7.4), 500 mM NaCl, 10% glycerol, 0.5% Nonidet P-40, 1.5 mM $MgCl_2$, 0.2 mM EDTA). The ChlR1 protein was eluted with 4 μg/ml 3 x FLAG peptide (Cat# F4799, Sigma) in buffer C (25 mM Tris HCl (pH 7.4), 100 mM NaCl, 10% glycerol, 0.1% Tween 20, 5 mM Tris (2-carboxyethyl) phosphine hydrochloride) (Sigma) for 1 h. Aliquots were frozen in liquid nitrogen and stored at -80°C. The concentrations of ChlR1 proteins were determined by Bradford (Bio-Rad) using bovine serum albumin (BSA) as a standard.

To express and purify the ChlR1 protein in bacteria, the human *ChlR1* gene was cloned into pET28a vector. Briefly, *E. coli* Rosetta 2 cells harboring the recombinant gene were grown at 37°C in LB medium containing 30 μg/mL kanamycin and 34 μg/mL of chloramphenicol until the A_{600} reached 0.6, induced by 1 mM IPTG at 16°C overnight and then the cells were harvested by centrifugation at 5,000 g for 10 min at 4°C; they were stored at -80°C until used. The cells were broken by sonication in buffer D (25 mM Tris pH 8.0, 0.15 M NaCl, 100 μM Tween 20 and 10% glycerol) with protease inhibitor (Roche Applied Science) and 1 mM phenylmethylsulfonyl fluoride (PMSF). The cell debris and inclusion bodies were removed by centrifugation at 45,000 g for 30 min at 4°C. The

supernatant was applied to Ni-NTA beads equilibrated with buffer A; washed with 10 column volume (CV) of wash buffer E (25 mM Tris pH 8.0, 0.5 M NaCl, 100 µM Tween 20 and 10% glycerol) containing 25 mM imidazole and eluted with 5 CV of elution buffer E containing 250 mM imidazole. The protein fractions were confirmed with SDS-PAGE; fractions with high protein yield were pooled and subjected to size-exclusion chromatography on a Sephacryl S-300 HR 16/60 (GE Healthcare) equilibrated with buffer D containing 0.1% β-mercaptoethanol. The fractions were collected at a flow rate of 0.5 mL/min with the same buffer. The protein was confirmed with SDS-PAGE and the fractions in the peak were pooled and concentrated.

3.4 Western Blot

Twenty micrograms of protein were denatured at 100°C for 5 min, then resolved on 10% polyacrylamide Tris-glycine SDS gels, and transferred to PVDF membranes. The membrane was blocked in PBS containing 5% powdered milk at room temperature for 1h, followed by probing with ChlR1 antibody, rabbit monoclonal anti-ChlR1 (1:2000, cat# H00001663-K, Abnova), or Flag antibody (1:5000, cat# A8592, Sigma), respectively. Goat anti-rabbit or goat anti-mouse IgG-horseradish peroxidase conjugate (cat# sc-2004, Santa Cruz Biotech) were used as secondary antibody at a 1:10,000 dilution and detected using ECL Plus (GE Healthcare).

3.5 Helicase Assay

The helicase assay reaction mixtures (20 µL) contained 40 mM Tris HCl (pH 7.4), 25 mM KCl, 5 mM $MgCl_2$, 2 mM dithiothreitol, 2% glycerol, 100 ng/µL bovine serum albumin, 2 mM ATP, 10 fmol of duplex DNA substrate, and the indicated concentrations of ChlR1. Helicase reactions were initiated by the addition of ChlR1 and incubated at 37°C for 30 min. Helicase reactions were terminated by addition of Stop buffer containing EDTA. Reaction products were resolved on nondenaturing 12% (19:1 acrylamide/bisacrylamide)

polyacrylamide gels for the forked duplex substrates as described previously (Wu *et al*., 2012a). Reactions were quenched with the addition of 20 µl of 2× stop buffer (17.5 mm EDTA, 0.3% SDS, 12.5% glycerol, 0.02% bromphenol blue, 0.02% xylene cyanol). For standard duplex DNA substrates, a 10-fold excess of unlabeled oligonucleotide with the same sequence as the labeled strand was included in the quench to prevent reannealing. Products of G4 unwinding reactions were resolved on 8% (19:1 acrylamide:bisacrylamide) polyacrylamide gels with 10 mm KCl in the gel and the running buffer. Radiolabeled DNA species in polyacrylamide gels were visualized using a PhosphorImager and quantitated using Quantity One software (Bio-Rad).

3.6 Electrophoretic Mobility Shift Assay (EMSA)

Protein/DNA binding mixtures (20 µL) contained the indicated concentrations of ChlR1 and 10 fmol of the specified ^{32}P-end-labeled DNA substrate in the same reaction buffer as that used for helicase assays (see above) without ATP. The binding mixtures were incubated at room temperature for 30 min after the addition of ChlR1. After incubation, 3 µL of loading dye (74% glycerol, 0.01% xylene cyanol, 0.01% bromphenol blue) was added to each mixture, and samples were loaded onto native 5% (19:1 acrylamide/bisacrylamide) polyacrylamide gels and electrophoresed at 200 V for 2 h at 4°C using 1×TBE as the running buffer. The resolved radiolabeled species were visualized using a PhosphorImager and analyzed with Quantity One software (Bio-Rad).

3.7 ATP Hydrolysis Assays

ATP hydrolysis was measured using [γ-^{32}P]ATP (PerkinElmer) and analysed by thin-layer chromatography (TLC) on polyethyleneimine-cellulose plates (J.T. Baker).The standard reaction mixture (20 µL total volume) contained 25 mM Hepes-NaOH (pH 7.5), 25 mM potassium acetate, 1 mM magnesium acetate, 1 mM DTT, 100 µg/ml bovine serum albumin, 250 µM [γ-^{32}P] ATP, 60 nM ChlR1 protein, and was incubated at 37°C. Reactions were

quenched with 50 mM EDTA final concentration. The reaction mixture was spotted onto a PEI-cellulose TLC plate and resolved by using 0.5 M LiCl, 1 M formic acid as the carrier solvent. The TLC plate was exposed to a phosphorimager cassette for 1 h and visualized using a Phosphor-Imager and analyzed with Quantity One software (Bio-Rad).

For experiments to determine K_M (ATP), the concentration of M13mp18 ssDNA was 2.1 nM, the concentration of ATP ranged from 31 to 4000 μM, and the reaction was incubated for 30 min. For determination of Kcat, the concentration of ATP was 8.5 mM. 5 μL aliquots were removed and quenched with 5 μL of 0.1 M EDTA at 0, 7.5, 15, 30, 45 min, respectively. The kinetic parameters were calculated by Enzyme Kinetics 1.3 (SigmaPlot, Systat Software Inc) using the Michaelis-Menton equation. All experiments were repeated at least three times.

3.8 ATP Binding Assay Using Chromatography

The ATP binding assay (30 μL) was performed in the same reaction buffer for the helicase or ATPase assay described above with 5 μCi [α-^{32}P] ATP (3000 Ci/mmol, PerkinElmer). Assays were initiated by adding ChlR1 protein to a final concentration of 230 nM, followed by incubating at 4°C for 30 min. Reactions were then applied to Bio-Spin P30 Tris chromatography columns (Bio-Rad), which had been pre-equilibrated in a reaction buffer. One drop (~45 μL) fractions were collected as flow-through under gravity with TE. The specific radio activity of each fraction was determined by a liquid scintillation counter (Beckman LS 6000TA). The first peak (3-4 drops) was considered as protein-bound ATP, and the second peak as unbound ATP.

3.9 ATP Binding Assay Using Agarose Beads

An ATP AffiPur kit was obtained from Jena Bioscience (Cat# AK-102, Jena) containing four types of ATP-agarose: [a] Aminophenyl-ATP-Agarose, [b] 8-[(6-Amino)hexyl]-amino-ATP-agarose, [c] N6-(6-Animo)hexyl-ATP-agarose and [d]

2'/3'-EDA-ATP-Agarose.

ATP assays were performed according to the manufacturer's protocol. 100 µg of purified protein was incubated with 50 µL of each ATP-agarose beads suspension for 2 h at 4°C. The resulting beads were washed 3 times with 500 µL of wash buffer each time, and bound protein was eluted by adding SDS–PAGE sample buffer and heating for 10 min at 98°C. The supernatants were subjected to Western blot analysis using anti-FLAG antibody (Sigma).

3.10 Size Exclusion Chromatography

Purified recombinant ChlR1 protein was applied to a Sephacryl S-300 HR size exclusion column (GE Healthcare) using an AKTApure system (GE Healthcare) that was pre-equilibrated with 25 mM Tris·HCl (pH 7.5), 10% glycerol, 0.15 M NaCl, 1 mM EDTA, and 0.5 mM DTT. The protein was eluted with same buffer at a rate of 0.1 ml/min, and 0.5-ml fractions were collected. Proteins were detected using a UV detector. The column was calibrated using standard molecular mass markers: thyroglobulin (669 kDa), apoferritin (443 kDa), beta amylase (200 kDa), alcohol dehydrogenase (150 kDa), and albumin (66 kDa, all from Sigma).

3.11 Thermal Stability Shift Assay (TSA)

All reactions were incubated in a 30 µL final volume and assayed in 96-well plates using 20 x SYPRO Orange (cat# S-6651, Invitrogen) and 1 µM purified ChlR1 protein. Protein elution buffer was added instead of protein in the control samples. The plates were sealed with Optical-Quality Sealing Tape (Bio-Rad). Thermal melting experiments were carried out using a StepOnePlus Real-Time PCR System (Applied Biosystems) melt curve program with a ramp rate of 1°C and temperature range of 25°C to 60°C. Melting temperature (T_m) is defined as the midpoint of temperature of the protein-unfolding transition. T_m was calculated by fitting the sigmoidal melt curve to the Boltzmann equation, with R2 values

of >0.99.

3.12 Proteolysis Mapping

An equal amount of ChlR1-WT or ChlR1-Q23A protein (300 nM) was used in digestion reactions (20 μL), and incubated at room temperature for 3 min with a range of trypsin concentrations (0-200 nM, Sigma). Reactions were stopped by the addition of 10 μL of SDS–PAGE gel loading buffer, and electrophoresised on a 10% SDS–PAGE followed by Western blotting using an anti-FLAG antibody (Sigma).

3.13 Steady-state Fluorescence Depolarization

Steady state fluorescence depolarization (rotational anisotropy) was used to measure enzyme-DNA binding affinities using the same fluorescence labeled forked dsDNA substrates (**Table 1**) that were used for helicase assays. Measurements were performed in a quartz cuvette of 1 cm path length. Reactions were 70 μL and contained fluorescence-labeled forked dsDNA (10 nM) in binding assays buffer and ChlR1-WT (0-1900 nM) and ChlR1-Q23A (0-2300 nM) were titrated into the reaction. A QuantaMaster QM-4 spectrofluorometer (Photon Technology International, NJ, USA) with a dual emission channel was used to collect data and calculate anisotropy. Measurements were made at 21°C. Samples were excited with vertically polarized light at 495 nm (6 nm band pass) and vertical and horizontal emissions were measured at 520 nm (6 nm band pass). Apparent dissociation constants (k_d) were obtained by fitting to a sigmoidal curve using Sigma Plot 11.2 software. The fluorescence anisotropy was calculated by the following equation, r is the observed anisotropy, $I_{\parallel}$ and $I_{\perp}$ stand for the intensity of the fluorescence polarized parallel and perpendicular to the excitation beam, respectively.

$$r = \frac{I_{\parallel} - I_{\perp}}{I_{\parallel} + 2I_{\perp}}$$

4. Results

4.1 Site Directed Mutagenesis of Glutamine to Alanine in the Q Motif of ChlR1

To understand the roles of the Q motif present in the ChlR1 helicase, the conserved glutamine was changed to alanine by QuikChange site-directed mutagenesis kit according to the manufacturer's instructions (Stratagene) using appropriate primers (**Table 1**) for the vector of pcDNA3. The ChlR1-Q23A mutation and construct were confirmed by direct DNA sequencing using the purified plasmid. Sequencing results confirmed that the invariant glutamine (CAG) had successfully changed to alanine (GCG) (**Fig.4.1**).

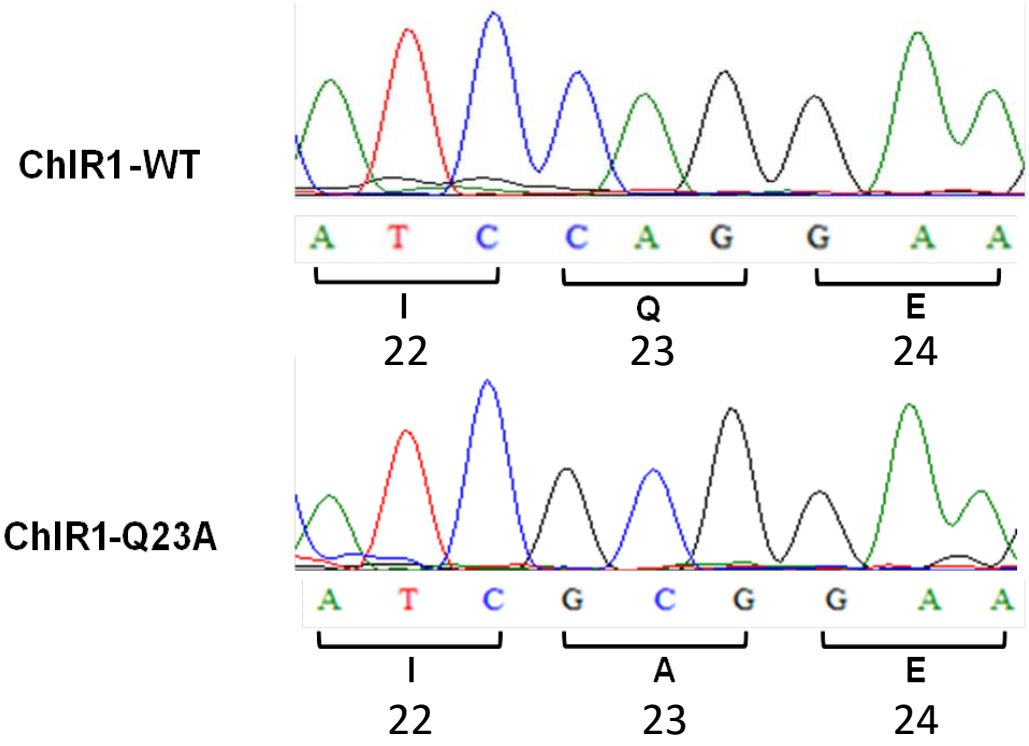

Fig. 4.1 The QA point mutation is confirmed by sequenceing. The change of glutamine (Q) to alanine (A) in ChlR1 gene was confirmed by sequencing.

4.2 Protein Overexpression and Purification

To determine the functions of the Q motif in ChlR1 protein, HEK 293T cells were transfected with ChlR1-WT and ChlR1-Q23A plasmid DNA separately using PEI. The recombinant ChlR1 proteins were purified using anti-FLAG affinity chromatography to

near homogeneity as judged by their appearance as single bands after electrophoresis on Coomassie-stained SDS-polyacrylamide gel (**Fig. 4.2A**). A Western blot assays were performed to confirm that the purified proteins were indeed ChlR1 using anti-FLAG antibody (**Fig. 4.2B**) and anti-ChlR1 antibody (**Fig. 4.2C**). Protein degradation bands can be observed at 75 kDa region, and the Q23A protein is more unstable compared to wild-type protein. We also purified an ATPase dead mutant ChlR1-K50R protein (data not shown) in which the invariant lysine residue was replaced with arginine (Guo *et al*., 2015).

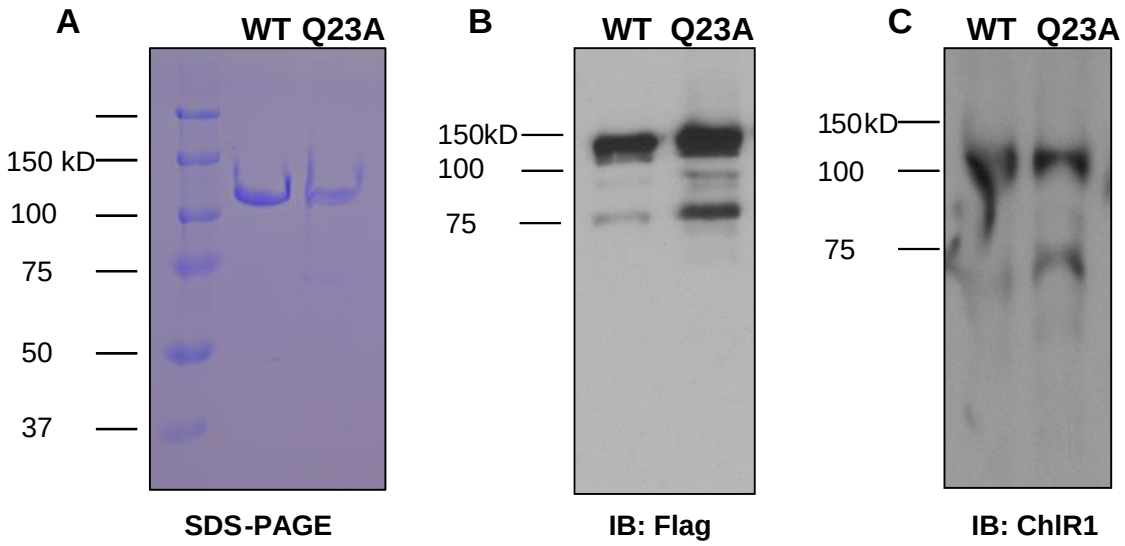

Fig. 4.2 Purification and identification of ChlR1 proteins. (**A**) ChlR1 proteins were purified and electrophoresed on Coomassie-stained SDS-polyacrylamide gel. (**B** and **C**) Western-blot analysis of the purified proteins with anti-FLAG antibody (**B**) and anti ChlR1 antibody (**C**) respectively.

4.3 The ChlR1-Q23A Protein Abolishes Helicase Activity

Although ChlR1 plays a role in the establishment of sister chromatid cohesion during replication, it is not well understood how the helicase functions in this capacity. Using a forked duplex DNA substrate that we know ChlR1-WT can efficiently unwind (Wu *et al*., 2012a), we tested the helicase activity of ChlR1-Q23A. Helicase assays revealed that changing the invariant glutamine of the Q motif in ChlR1 into alanine abolished its helicase activity on forked duplex DNA (**Fig. 4.3A and 4.3B**). We also increased the incubation

time (60 min), ATP concentration (10 mM),and protein concentration (to 12 nM), but failed to detect any unwinding activity for ChlR1-Q23A (data not shown). The ATPase dead mutant ChlR1-K50R protein also failed to unwind the forked duplex DNA (**Fig. 4.3C**).

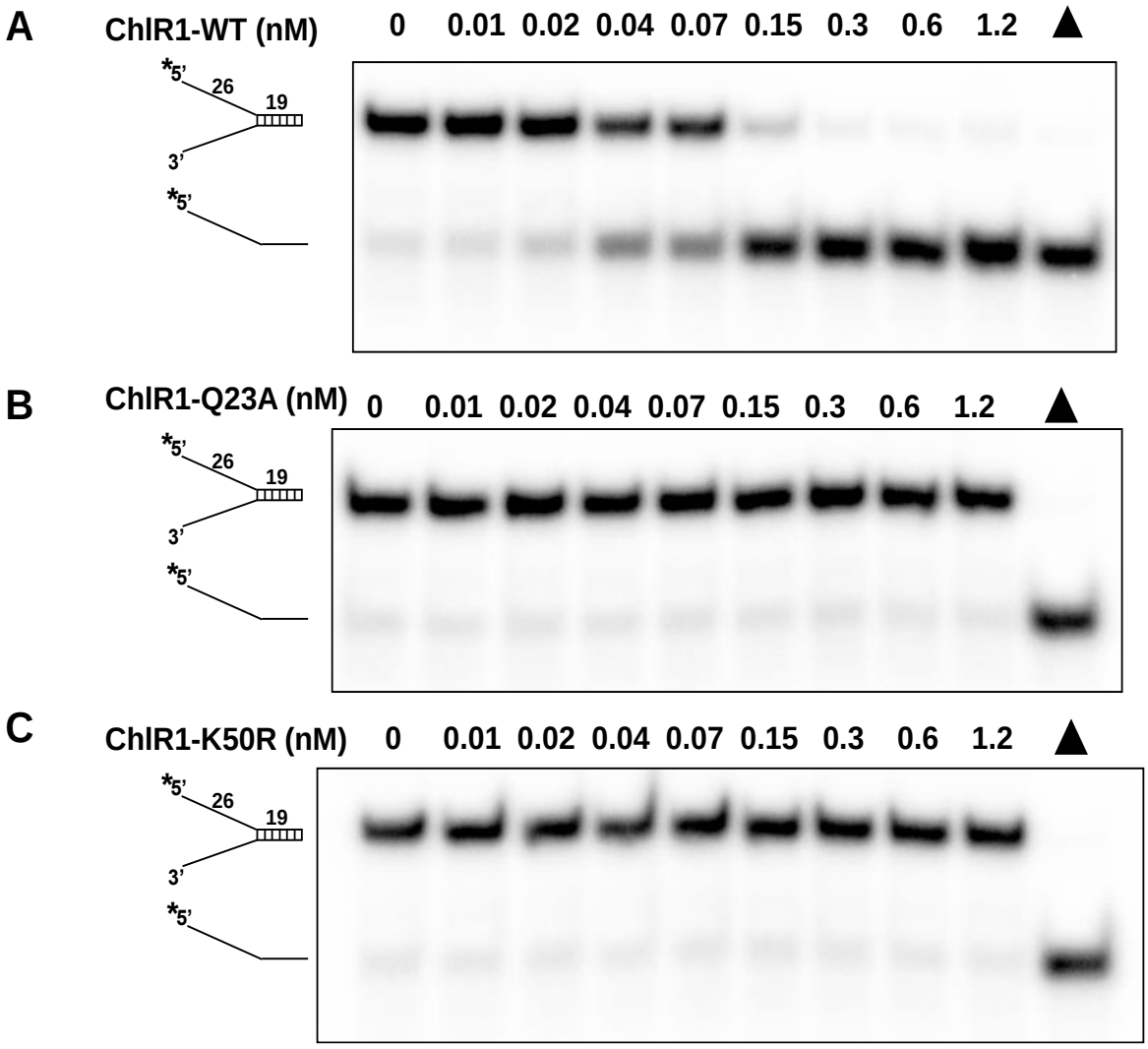

Fig. 4.3 Helicase analysis of the ChlR1-WT, Q23A and K50R. Helicase reactions were performed by incubating with indicated protein ChlR1-WT (**A**), ChlR1-Q23A (**B**), and ChlR1-K50R (**C**) concentration with 0.5 nM fork duplex DNA substrate at 37°C for 30 min. Helicase reactions were terminated by addition of Stop buffer containing EDTA. Reaction products were resolved on nondenaturing 12% (19:1 acrylamide/bisacrylamide) polyacrylamide gels and electrophoresed at 180 V for 2 h at room temperature using 1× TBE as the Running buffer. The filled triangle stands for heat-denatured DNA substrate control.

Alternate DNA structures such as G-quadruplex (G4) DNA that may impede the replication fork are proposed to form in G-rich regions that are quite abundant in the human genome (Maizels, 2006). To test this observation, ChlR1-Q23A was evaluated for the unwinding activity on a well characterized four-stranded parallel G4 substrate (TP-G4) and antiparallel G4 structure (OX-1 G2') that have been used before (Wu *et al*., 2008). Helicase assays on these two substrates showed ChlR1 had a strong preference for a two-stranded antiparallel G4 substrate (G2') (**Fig. 4.4A**), and was only marginally active on a four-stranded parallel G4 structure (**Fig. 4.4B**). Nevertheless, ChlR1-Q23A was inactive on both substrates.

Taken together, these results demonstrated that the Q motif in ChlR1 helicase is essential not only for forked duplex DNA binding, but also for two-stranded antiparallel G4 DNA binding.

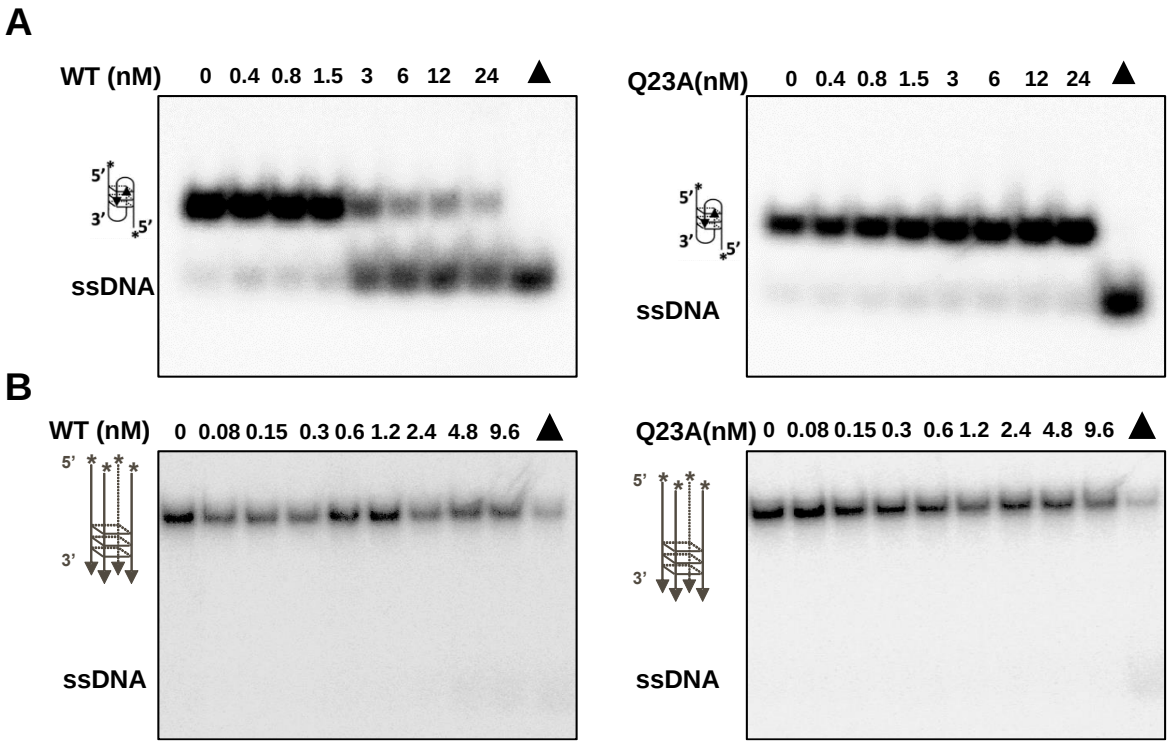

Fig. 4.4 Helicase analysis of ChlR1-WT and Q23A on G-quadruplex substrates. Representative image of the unwinding reaction on OX-1 G2' substrate (**A**) and TP-G4 substrate (**B**) with increasing protein concentration. Mobility of G4 DNA and single-stranded DNAs are indicated by the cartoons on the left. Triangle, heat-denatured DNA substrate control, form a weak band at the bottom of the gel.

4.4 The ChlR1-Q23A Protein Has Poor DNA Binding Ability

4.4.1 Electrophoretic Mobility Shift Assay (EMSA)

The ChlR1-Q23A mutant protein with no helicase activity might reflect an impaired DNA binding activity. To test this assumption, gel mobility shift assays were performed with ChlR1-WT and ChlR1-Q23A using the same radiolabeled DNA substrates that were used in the helicase assay. Results demonstrated that ChlR1-WT bound the DNA molecules in a protein concentration-dependent manner while ChlR1-Q23A protein's DNA binding ability was abolished (**Fig. 4.5A**). When the protein concentration was increased eight fold (96 nM), ChlR1-Q23A could bind weakly with the substrate (**Fig. 4.5B**). To address whether a conformal change induced by ATP binding would affect its nucleic acid binding, ChlR1-WT was incubated with AMP-PNP, a non-hydrolysable ATP analog, then with forked DNA substrate, and found its DNA binding activity was reduced (**Fig. 4.5C**). Thus, we concluded that the Q mutation affects ChlR1 proteins' fork duplex DNA binding ability.

To verify whether the loss of ChlR1-Q23A protein's G4 substrates unwinding ability is also due to the poor DNA binding ability, ChlR1-WT and Q23A protein's binding ability was also evaluated on TP-G4 and OX1-G2 substrates. EMSA results revealed that ChlR1-WT bound TP-G4 structure in a concentration dependent manner, but significantly less DNA binding activity was observed for ChlR1-Q23A (**Fig. 4.6A**). Similar results were observed on OX1-G2' substrate where the WT bound the substrate while the mutant bound poorly (**Fig. 4.6B**).

4.4.2 Steady-state Fluorescence Depolarization

Since the ChlR1-Q23A mutant protein has poor DNA binding ability with electrophoretic mobility shift assays, an alternative method, fluorescence rotational anisotropy was performed to determine the k_d value. Using the same forked duplex substrate **(Table 1)** that was used for EMSA, DNA was labeled with fluorescein, and a constant amount of DNA was incubated with increasing concentrations of protein (**Fig.4.7**).

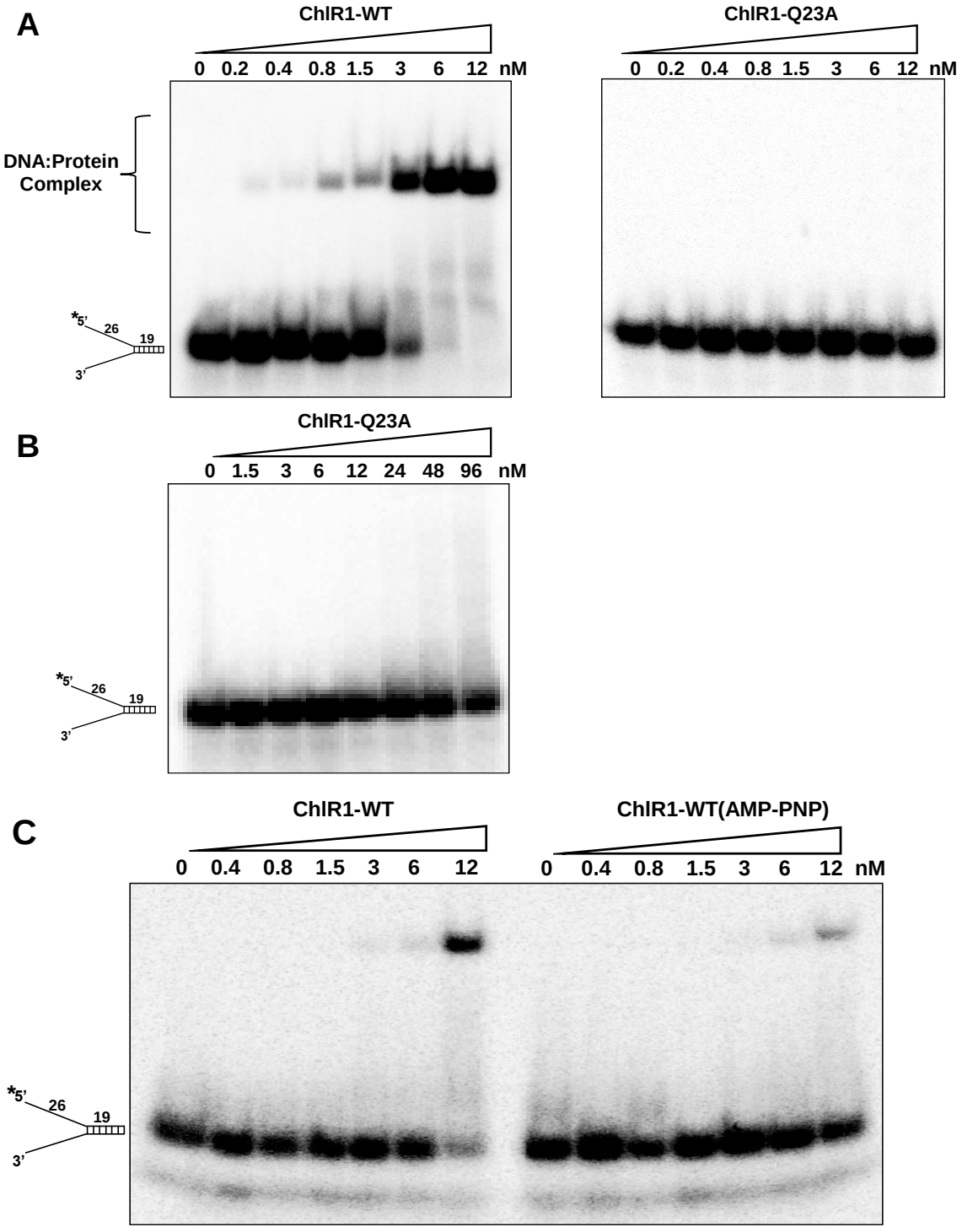

Fig. 4.5 Electrophoretic mobility shift assay of ChlR1 proteins with fork duplex DNA. The indicated concentrations of ChlR1 proteins (**A**, 0-12 nM; **B**, 0-96 nM) were incubated with 0.5 nM forked duplex DNA substrate at room temperature for 30 min under standard gel shift assay conditions. The DNA-protein complexes were resolved on native 5% polyacrylamide gels and electrophoresed at 200 V for 2 h at 4℃. (**C**) Gel shift assay was performed without (left) or with 2 mM AMP-PNP (right), all other procedures were the same.

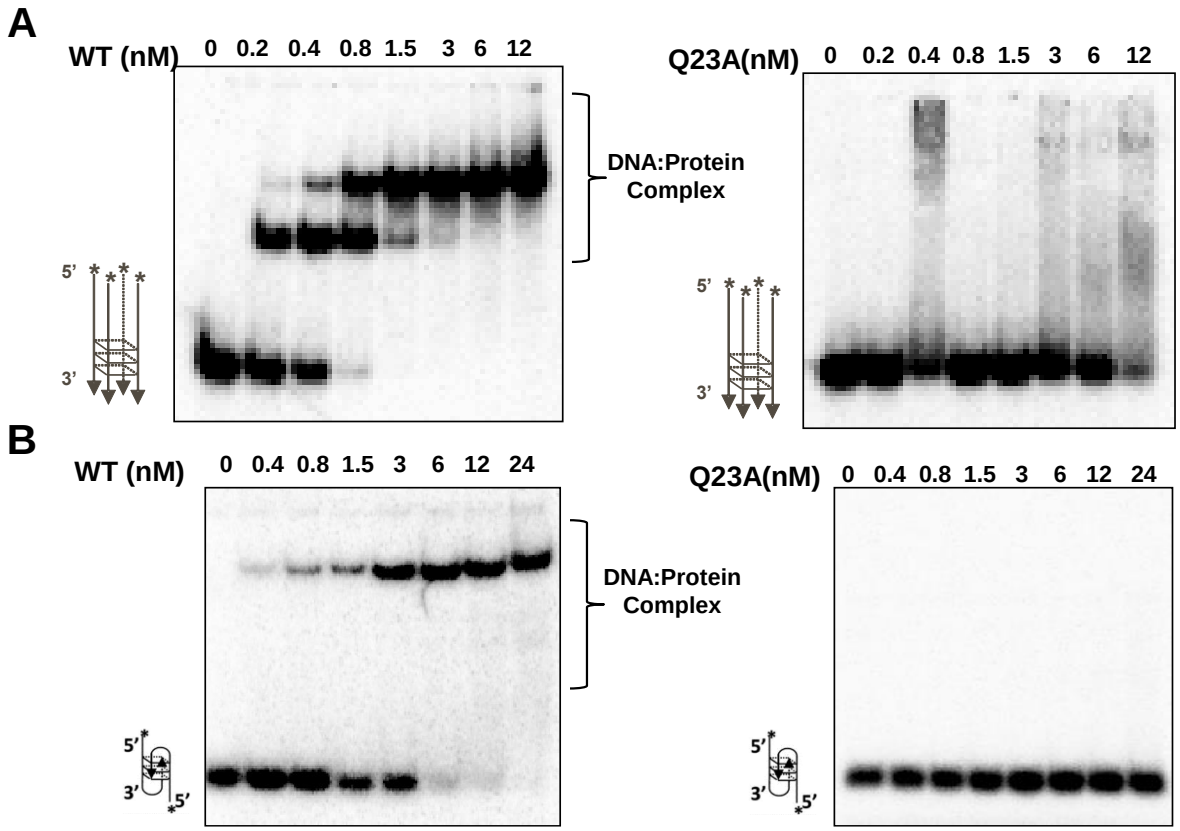

Fig. 4.6 Electrophoretic mobility shift assay of ChlR1 proteins with G4 substrates. Indicated concentrations of ChlR1 proteins were incubated with TP-G4 substrate (**A**) and OX1-G2' substrate (**B**) in the absence of ATP. The binding mixtures were incubated at room temperature for 30 min, then resolved on native 5% polyacrylamide gels. Mobility of the DNA and the DNA-protein complex are indicated on the left and right.

The apparent k_d for ChlR1-Q23A was 1000 nM, which is 2-fold higher than the k_d of ChlR1-WT (520 nM). Additionally, we performed filter binding assays (data not shown) of ChlR1 proteins with DNA and again determined the k_d values for WT of 105.5 nM, and for Q23A of 397.9 nM, further implicating that Q23A mutant has a reduced affinity for DNA. We also quantified the EMSA results, the k_d value for ChlR1-WT is 329 nM, but the k_d value for Q23A protein is too large to calculate. The DNA substrate concentration used in each experiment is different, which may cause protein-DNA binding affinity varies. Also the incubation time for EMSA assay is 30 mins, but for rotational anisotropy assay is only 1 min, so the k_d values for these experiments are not comparable.

When using same amount of fluorescence DNA substrate, the fluorescence rotational anisotropy curve usually will reach the same place after the binding is saturated, but the curves didn't saturate at the same anisotropy value in this experiment. There is possibility that more than one protein can load on a single DNA substrate and the loaded protein will change confirmation which maybe facilitate other protein's DNA loading process. If the assumption is real, when compared with ChlR1-Q23A protein, the ChlR1-WT protein can bind DNA substrate tighter and recruit more protein to load on it. Thus even at saturated protein concentration, Q23A mutant cannot load as many protein as ChlR1-WT helicase, then DNA/WT protein complex will be much heavier than DNA/Q23A protein complex. Therefore, even at saturated protein concentration, the DNA/WT complex will rotate much slower than the DNA/Q23A complex, and the anisotropy curves won't reach the same place.

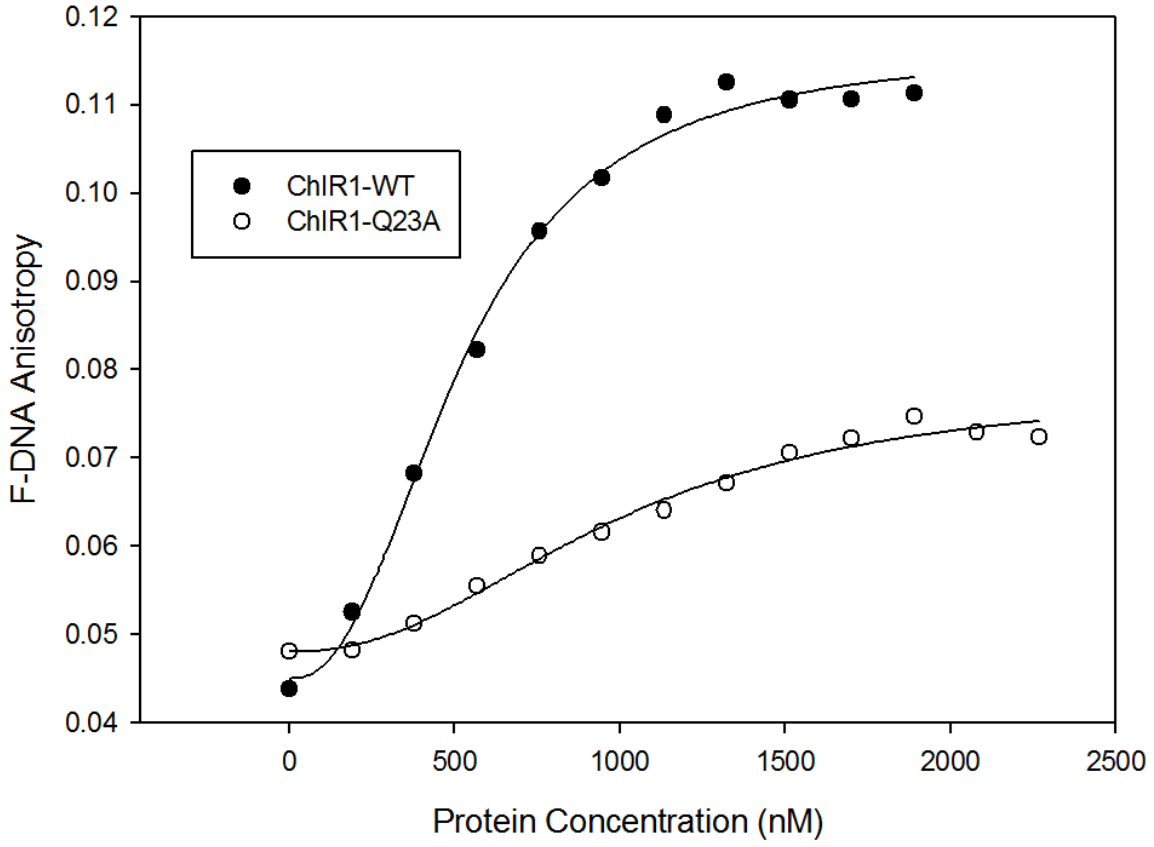

Fig. 4.7 Rotational anisotropy assays of ChlR1 proteins with forked duplex DNA. ChlR1-WT (0-1900 nM) and ChlR1-Q23A (0-2300 nM) were titrated into fluorescence -labeled forked dsDNA (10 nM) in binding buffer separately. Samples were excited with vertically polarized light at 495 nm and vertical and horizontal emissions were measured at 520 nm.

Taken together, these results demonstrated that the Q motif in ChlR1 helicase is essential for DNA binding, including forked duplex DNA and G4 DNA. These results also indicated that the loss of helicase activity of ChlR1-Q23A might be due to the poor binding ability between DNA and the helicase.

4.5 The ChlR1-Q23A is Impaired for ATP Hydrolysis but Retains ATP Binding Ability

4.5.1 ChlR1-Q23A Has Impaired ATP Hydrolysis

Usually, helicases can hydrolyze ATP in a DNA or RNA dependent manner to provide energy for unwinding activity. Thus the DNA-dependent ATPase activity of ChlR1-Q23A was compared with ChlR1-WT. Using covalently closed M13 single strand DNA as the effector molecule, the K_M value of ATP hydrolysis for ChlR1-WT was determined as 329.6 μM. Because of the very low ATPase activity, ChlR1-Q23A's K_M values could not be determined (**Fig. 4.8A**). Using an ATP concentration (8.5 mM) that was ~25-fold greater than the K_M for ChlR1-WT, ATPase activity was measured for ChlR1-WT and ChlR1-Q23A, and the *K*cat values for these two proteins were 1026 and 61 s^{-1} respectively (**Fig. 4.8B**). These results suggest that the ChlR1-Q23A mutant seriously compromises the ability of ChlR1 to hydrolyze ATP in a DNA-dependent manner.

4.5.2 The Conserved Q motif is not Important for ATP Binding

Next, we asked whether ChlR1-Q23A was able to bind ATP. To compare ATP binding by ChlR1-Q23A with ChlR1-WT, an equal amount of ChlR1-Q23A or ChlR1-WT protein was incubated with [α-^{32}P] ATP under identical conditions, and binding mixtures were analyzed by gel filtration chromatography (**Fig. 4.8C**). Scintillation counting of the eluted fractions demonstrated that ChlR1-Q23A bound ATP with similar affinity as ChlR1-WT. One pmol of ChlR1-WT bound 11.6 fmol ATP, while ChlR1-Q23A bound 10.1 fmol ATP (**Fig. 4.8D**). Using [α-^{32}P] ATP followed by gel filtration chromatography, we found that the

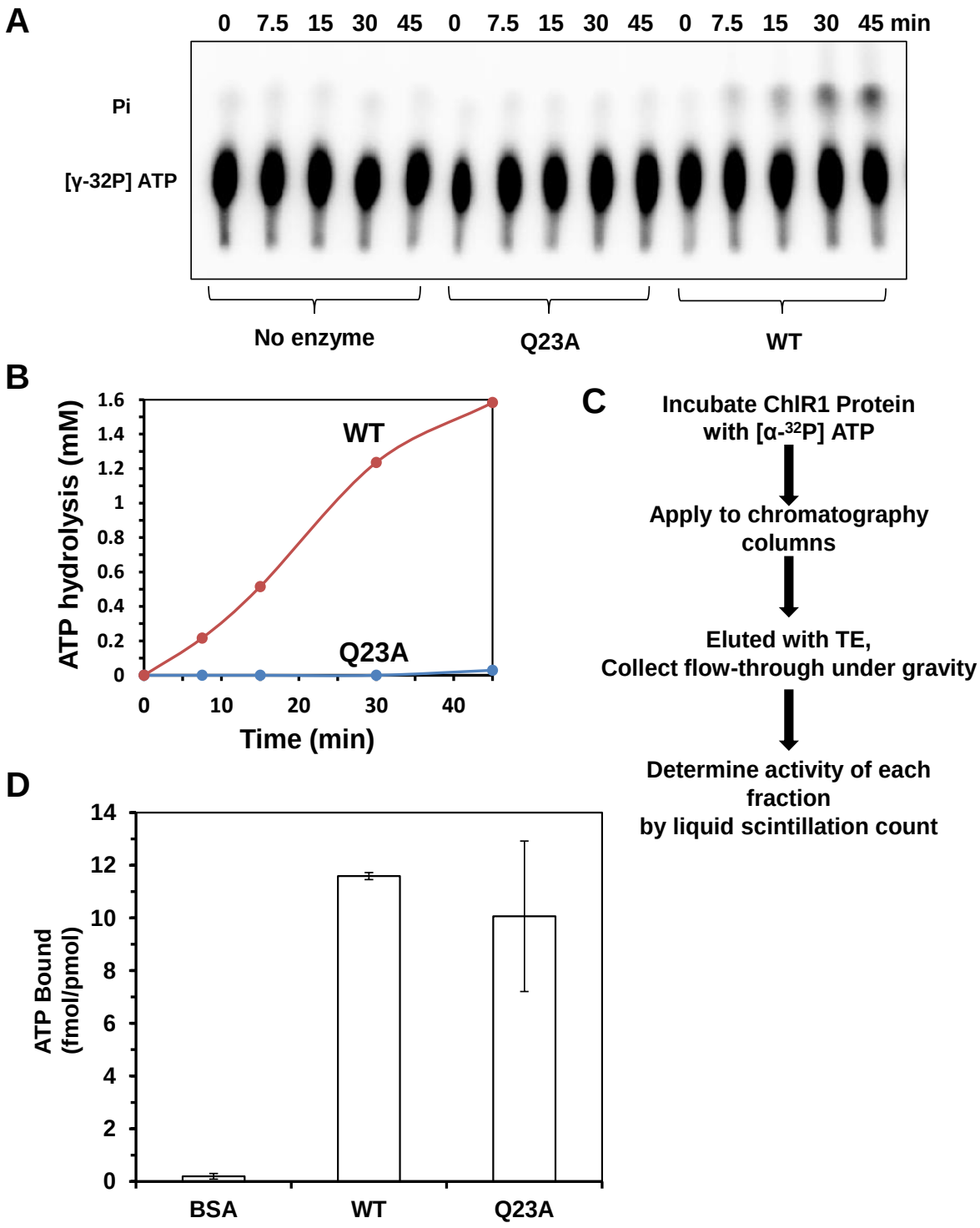

Fig. 4.8 ATP hydrolysis and binding analysis of ChlR1 proteins. (**A**) A Representative TLC plate showing ATP hydrolysis activity of WT and mutant. (**B**) The ATPase activity of WT and mutant Q23A was assayed as described in "Experimental Procedures" and is plotted as a function of time. (**C**) The flow chart of ATP binding experimental procedure. (**D**) Result of ATP binding assay. BSA serves as a negative control. Data represent the mean of at least 3 independent experiments, with SD indicated by error bars.

ChlR1-Q23A mutant protein can bind ATP with similar affinity as ChlR1-WT. In order to verify this result, an ATP AffiPur kit was used to test the mutant protein's ATP binding ability. This kit contains four types of ATP-agarose: Aminophenyl-ATP-agarose, 8-[(6-Amino) hexyl]-amino-ATP-agarose, N6-(6-Animo) hexyl-ATP-agarose, and 2′/3′-EDA-ATP-agarose. After screening the binding affinity of these four beads, Aminophenyl-ATP-agarose and N6-(6-Animo) hexyl-ATP-agarose were found to be better than the other two at binding ChlR1 protein, thus these two were used in the following experiments. The same amount of ChlR1-WT or Q23A proteins were incubated with ATP-agarose beads. It revealed that similar amounts of WT and Q23A proteins were retained on the ATP beads as were detected by Western blot (**Fig. 4.9**).

From these results, we concluded that ChlR1-Q23A bound ATP similar to ChlR1-WT but did not efficiently hydrolyze the nucleotide in the presence of a DNA effector.

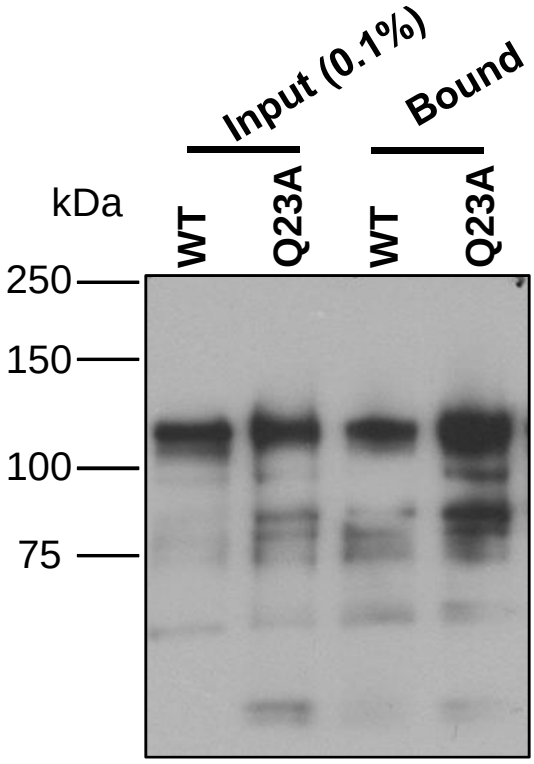

Fig. 4.9 Western blot of ChlR1 proteins retained by ATP-agarose. ATP binding by ChlR1 proteins was determined by AffiPur kit (Jena Bioscience) as described under "Experimental Procedures", followed by Western blot with an anti-FLAG antibody. 0.1% of input protein was loaded on gel as controls.

4.6 The ChlR1-Q23A Mutation Abolishes Translocase Activity

DNA triplex displacement experiments have been utilized to monitor the translocase activity of helicases, such as AddAB, FANCM, and PICH (Gilhooly and Dillingham, 2014; Meetei *et al.*, 2005; McClelland *et al.*, 2005; Biebricher *et al.*, 2013). In this assay, a triple helix is formed in which each nucleotide of the third strand forms Hoogsteen base pairs with Watson-Crick base pairs of the duplex. When the translocase proceeds through the triplex, it displaces the third strand. We found that wild-type ChlR1, but not the Q23A mutant, exhibited triple-helix displacement activity (**Fig. 4.10A and B**). Under the same reaction conditions, ChlR1-WT was also able to translocate along a short triplex structure (named flush triplex) which was constructed by annealing the same pyrimidine motif third strand (TC30) to a 30 bp duplex fragment, but the mutant ChlR1-Q23A failed (**Fig. 4.10C and D**). Together, these results suggest that ChlR1 can dissociate DNA triplex; however, the Q23A mutant has no translocase activity.

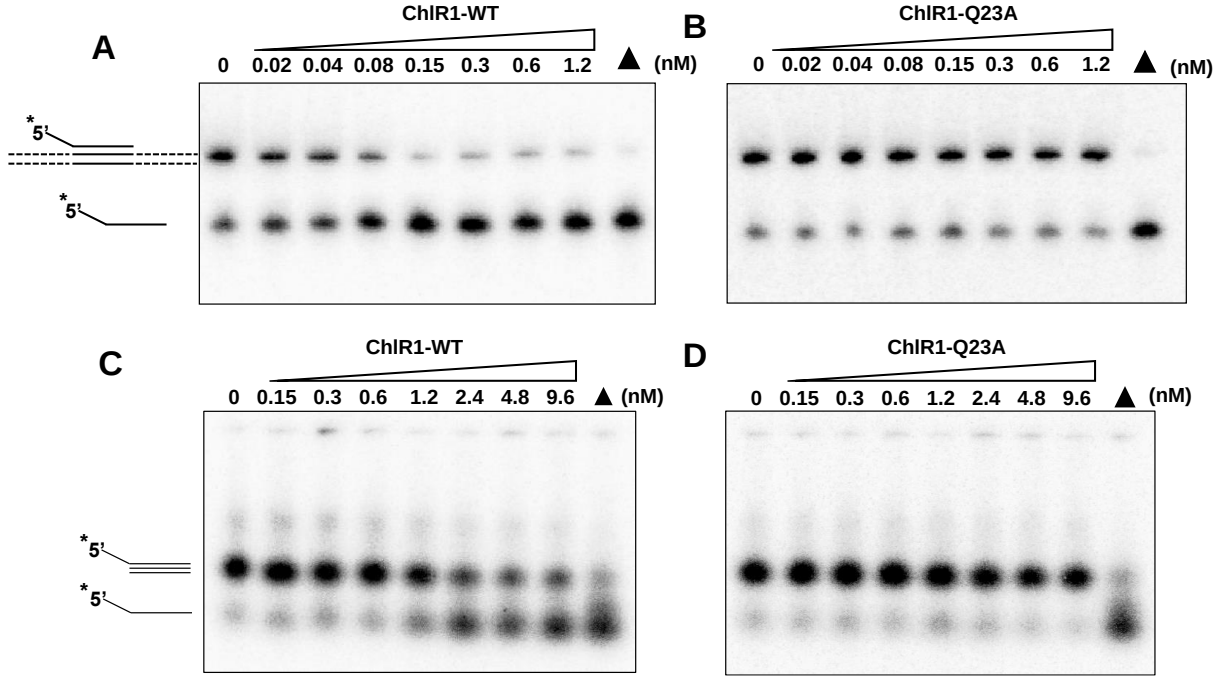

Fig. 4.10 ChlR1-Q23A fails to translocate on DNA triple helixes. Translocase activity reactions (20 μl) were performed by incubating the indicated ChlR1-WT (**A** and **C**) or ChlR1-Q23A (**B** and **D**) concentrations with 0.5 nM 5' tail plasmid-triplex substrate (**A** and **B**) or 5' tail flush triplex substrate (**C** and **D**) at 37 °C for 20 min under standard helicase assay conditions as described under "Experimental Procedures". Triangle is heat-denatured DNA substrate control.

4.7 The ChlR1-Q23A Has Similar Globular Structure with ChlR1-WT

4.7.1 The ChlR1-Q23A Has a Similar Melting Point (T_m) Value as ChlR1-WT

Thermal shift assays are widely used to measures the thermal stability of a target protein (Cavlar *et al*., 2013; Sainsbury *et al*., 2011; Hajer *et al*., 2014), which indirectly reflects protein folding. To rule out artifacts due to misfolding or instability of ChlR1-Q23A, thermal shift assays were performed for the purified recombinant ChlR1 proteins. In the temperature range of 25°C to 60°C, it has been found that ChlR1-Q23A protein exhibited a similar transition curve as the wild-type protein (**Fig. 4.11A**). The melting curve showed that the midpoint value (T_m) for ChlR1-WT and ChlR1-Q23A were both at 43.9°C (**Fig. 4.11B**), suggesting that ChlR1-Q23A protein's globular structure is similar to ChlR1-WT.

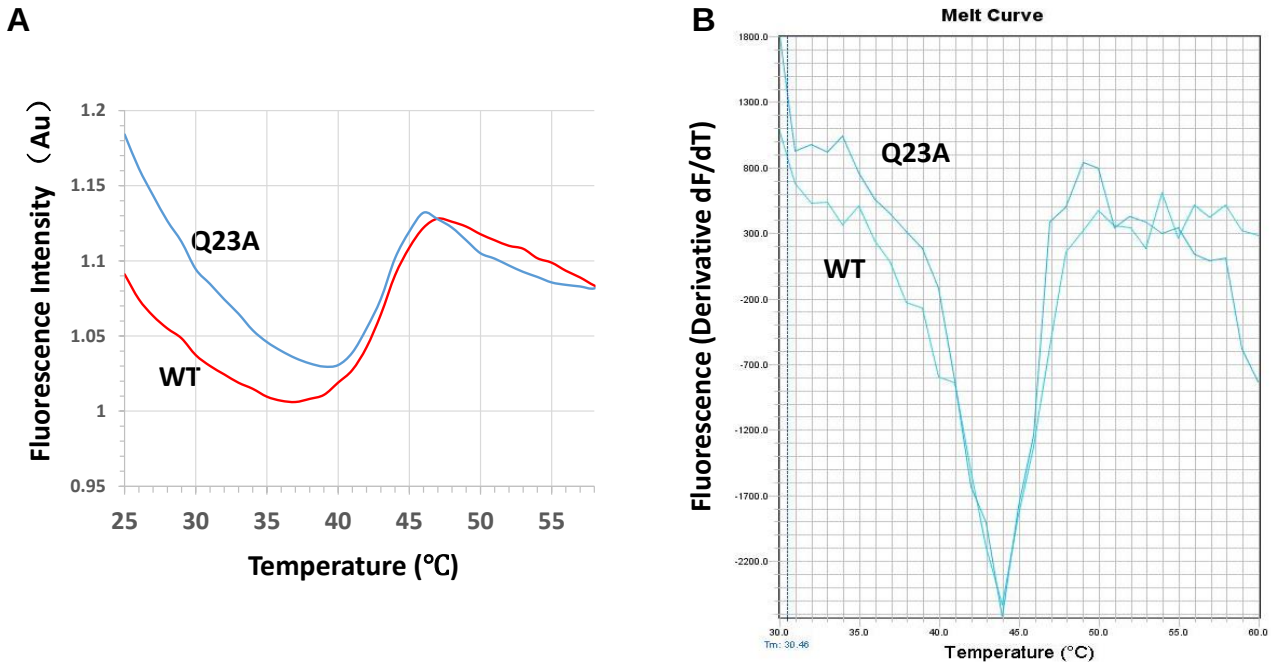

Fig. 4.11 Thermal stability assays of ChlR1 proteins. (**A**) Unfolding curves of ChlR1-WT and ChlR1-Q23A under temperature range of 25-60°C. (**B**) Derivative fluorescence melt curves that generated by StepOne Software v2.1.

4.7.2 Partial Proteolysis Mapping Revealed that ChlR1-Q23A Has Subtle Conformational Differences

Partial proteolysis mapping can be successfully used to probe conformational features of

proteins (Trkulja *et al*., 2014; Lamberti *et al*., 2005) The flexible sites and the unfolded polypeptide can be probed by proteolytic enzymes (Fontana *et al*., 2004). In order to gain insight into the subtle conformational changes that may be caused by the Q23A mutant, partial proteolysis mapping was used to probe the physical architecture of ChlR1 proteins. With an increasing concentration of trypsin, both ChlR1-WT and Q23A yielded some stable fragments around 75, 50 and 13 kDa, but ChlR1-Q23A yielded fragments around 37 kDa that were not present in the wild type ChlR1 protein (**Fig. 4.12**). These results suggested that even though ChlR1-WT and ChlR1-Q23A have similar globular structure; there is still some subtle conformational difference between these two proteins, which may be caused by the Q23 residue substitution.

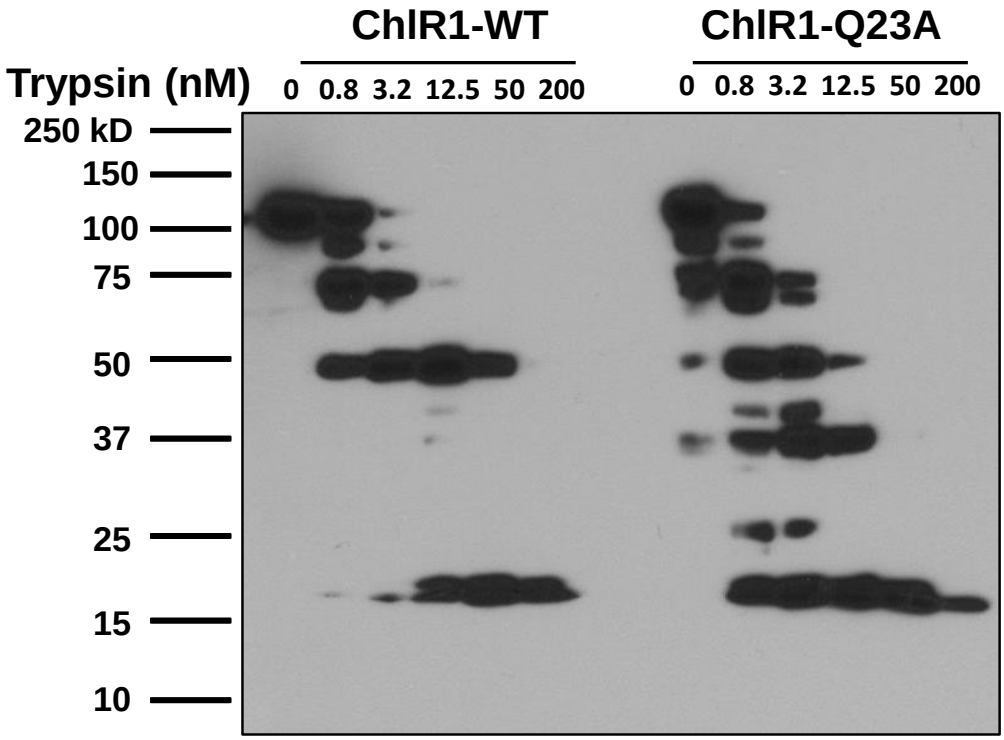

Fig. 4.12 Representative image of partial proteolysis mapping of ChlR1 proteins. ChlR1 proteins (WT and Q23A, 100 nM each) were digested with increasing concentration of trypsin, protein fragments were separated on SDS–PAGE, followed by Western blot analysis using an anti-FLAG antibody.

4.8 The ChlR1 Protein Exists as a Monomer in Solution

Many helicases self-assemble to form dimers or higher order oligomers that can influence

their catalytic or biological functions (Singleton *et al*., 2007; Lohman and Bjornson, 1996). Oligomerization is an important property of SF1 and SF2 helicases (Patel and Donmez, 2006). N- and C-terminal domains can influence or even define the function of a helicase through promoting oligomerization (Klostermeier and Rudolph, 2009). For example, SF2 helicase FANCJ functions as a dimer in solution and the Q motif in FANCJ regulates dimerization (Wu *et al*., 2012b). To determine whether the Q motif might affect oligomerization of ChlR1, wild-type ChlR1 protein was analyzed by size exclusion chromatography. The purified ChlR1-WT protein (**Fig. 4.13A**) was applied on a Sephacryl S-300 HR column, and a major peak was detected at an elution volume of ~65 mL (**Fig. 4.13B**). Using protein standards, a calibration curve was generated as shown in **Fig. 4.13C**.

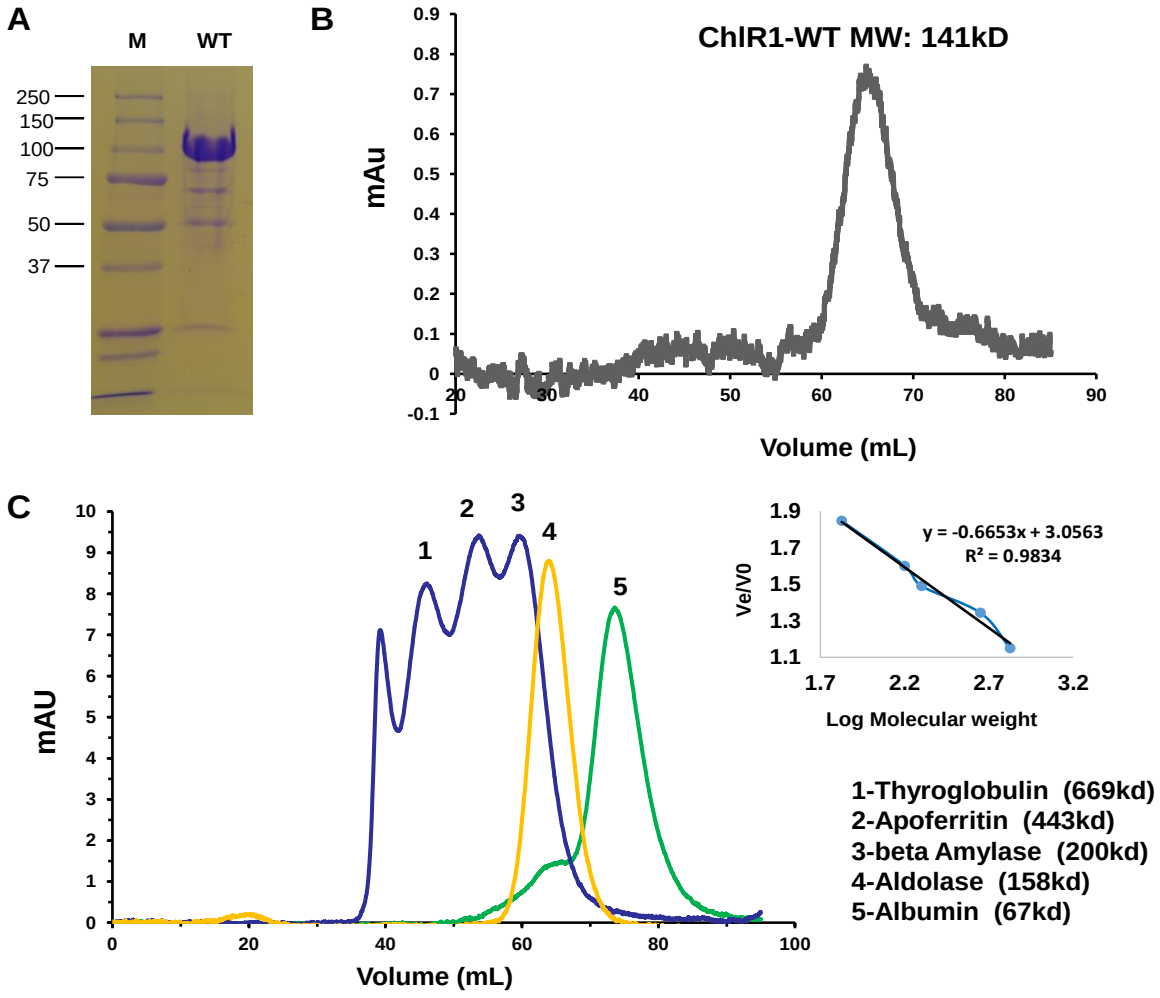

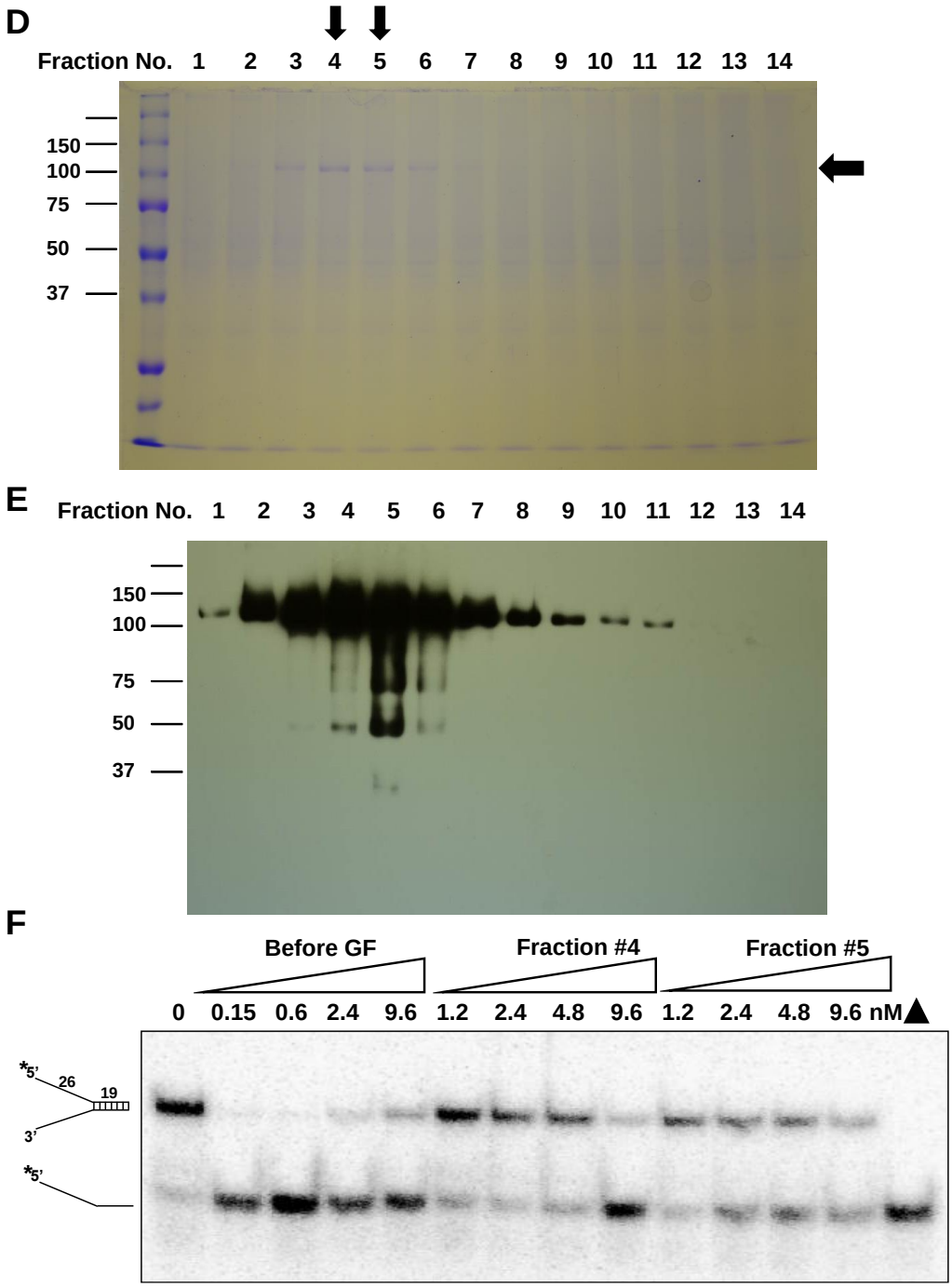

Fig. 4.13 ChlR1 protein oligomerization state determination. (**A**) Coomassie blue stained SDS-PAGE gel showing the ChlR1 protein. (**B**) Chromatographic profiles of ChlR1 protein. (**C**) Chromatographic profiles of standard proteins on a HiPrep 16/60 Sephacryl S-300 HR column. The equation of protein molecular mass was showed in right up corner. (**D**) Fourteen fractions were picked from the peak area and analyzed by 10% SDS-PAGE, followed by Coomassie Blue staining. (**E**) The fractions in D were immunoblotted with an anti-FLAG antibody. (**F**) Fractions No.4 and No.5 were subjected to helicase assay with a fork duplex DNA. Before gel filtration (GF) was used a positive control. Filled triangle, heated denature samples.

According to the calibration curve, the molecular weight of this peak was determined as 140 kDa, which is close to ChlR1's expected mass (110 kDa). The fractions from the peak region on SDS-PAGE (**Fig. 4.13D**) and Western-blot assays with anti-ChlR1 antibody (**Fig. 4.13E**), demonstrated that the absorption peak was contributed by ChlR1 protein. The fraction #4 and #5 used in SDS-PAGE were further analyzed for helicase activity (**Fig. 4.13F**). The ChlR1 protein collected before SEC exhibited higher unwinding activity than fraction #4 and #5 that were collected after SEC, which might be due to the over-night size exclusion chromatography procedure that reduced the protein's helicase activity.

4.9 Expression and Purification of ChlR1 Protein from Bacteria

For ChlR1 protein production, the expression level is limited in human cells and the cost is high. In order to obtain a larger amount of protein at low cost, we attempted to overexpress and purify ChlR1 protein from *E. coli*. To this end, *ChlR1* gene was cloned into a pET28a vector, and protein production was induced by IPTG in 1L *E. coli*. The soluble extract of His-tagged ChlR1 protein was first purified by Ni-NTA column chromatography. SDS-PAGE analysis of purified protein showed that fractions 4 and 5 had the highest protein concentration (**Fig. 4.14A**). Thus, fractions 4 and 5 were loaded on a HiPrep 16/60 Sephacryl S-300 HR column, and SEC revealed that the ChlR1 protein eluted as two major peaks (**Fig. 4.14B**). The first peak corresponded to a higher oligomerization state with an estimated size of 470 kDa, while the second peak corresponded to 119 kDa, suggesting that ChlR1 protein purified from bacteria can form tetramers and monomers in solution, but the ChlR1 protein expressed in human cells can only form monomer. Maybe due to the bacterial protein expression level is much higher than the human cell, so the protein has better oppotunities to form oligomers. Four fractions from each peak were selected to conduct the helicase assay. Interestingly we found that the ChlR1 tetramer has higher helicase activity than its monomer (**Fig. 4.14C**). We tried to purify the ChlR1-Q23A protein, but failed, because of protein aggregation.

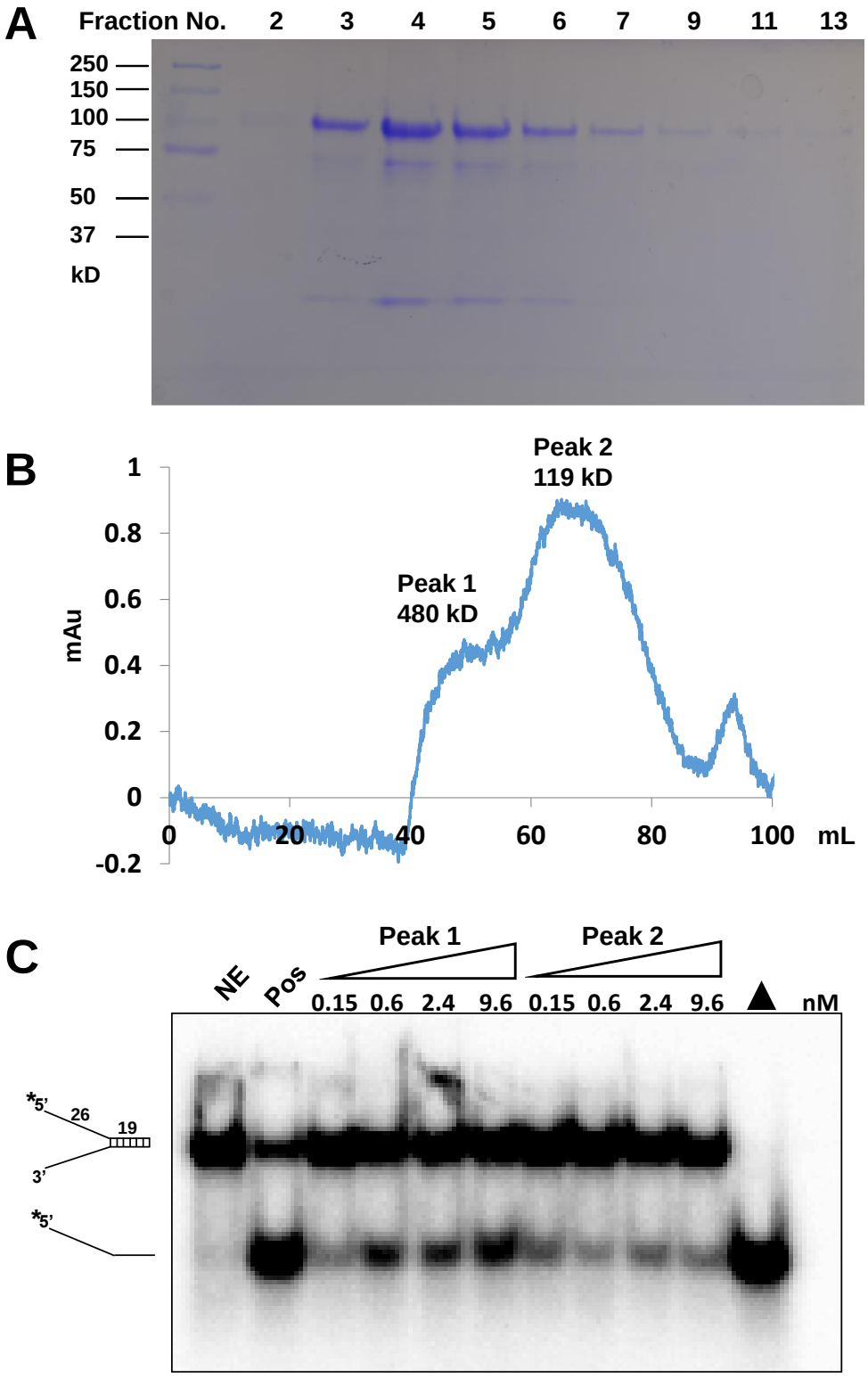

Fig. 4.14 Characterization of ChlR1 protein purified from bacteria. (**A**) SDS-PAGE analysis of ChlR1 protein purified from *E. coli* with Ni-NTA column. (**B**) Gel chromatography profile of ChlR1 protein. (**C**) Helicase assay of four fractions from two peaks in ChlR1 gel filtration profile (panel B). NE, no enzyme; pos, ChlR1 protein purified from human cells, used as a positive control; filled triangle, heated sample.

5. Discussion

In this study, we have discovered that the ChlR1-Q23A mutant abolished the helicase activity of ChlR1, and displayed reduced DNA binding ability. The mutant showed impaired ATPase activity but displayed normal ATP binding. A thermal shift assay revealed that ChlR1-Q23A has a similar melting point value as ChlR1-WT. Partial proteolysis mapping demonstrated that ChlR1-WT and Q23A have similar globular structure; although there is some subtle conformational difference between these two proteins. The ChlR1-Q23A mutation also abolished ChlR1's translocase activity. Taken together, we concluded that the Q motif is involved in DNA binding but not ATP binding in ChlR1 helicase.

5.1 The Presence and Functions of the Q Motif

The function of the Q motif has been shown to regulate ATP binding, ATP hydrolysis, and RNA binding. Using malachite green in the colorimetric ATPase assays to measure free phosphate, Tanner *et al.* found that the Q motif mutant in eIF4A has reduced ATP hydrolysis activity (Tanner *et al*., 2003). Howerve, they also crosslinked ^{32}P-ATP with the protein to detect the ATP binding ability and found that the Q motif mutant protein has 3-fold higher ATP binding ability than the wild-type protein. Nongkhlaw *et al* (2012) mutated the Q motif in SWI2/SNF2 protein SMARCAL1 and detected the ATP bydrolysis activity as well as ATP binding ability in the presence of DNA substrate. Their results suggested that motif Q is just required for ATP hydrolysis but not for ATP binding (Nongkhlaw *et al*., 2012). By using EMSA assays, Cordin *et al* (2004) found that the Q motif mutation in DEAD-box RNA helicases could effect the RNA substrate binding ability (Cordin *et al*., 2004). Therefore, the functions of Q motif remain inconsistent. We started biochemical characterization of ChlR1 and the results suggested that the Q motif in ChlR1 helicase has an essential role in DNA binding but not ATP binding.

Motif Q is also called motif 0, indicating it is a part of the conserved helicase core

elements along with seven helicase motifs (I, Ia, II–VI). In fact, experimental evidence had shown that the Q motif is in the minimal functional unit of the DEAD-box core (Banroques *et al*., 2011). In our study, replacement of the conserved glutamine with an alanine affects DNA binding in addition to ATP hydrolysis of ChlR1. However, compared with the other conserved seven helicase motifs, the Q motif is somewhat less conserved among SF2 helicases (Fairman-Williams *et al*., 2010). This motif is absent in the DEAH/RHA and viral DExH proteins, and these enzymes are not specific for adenosine triphosphates. For example, alanine-scanning mutagenesis has shown that motifs Q, Ia and Va are not essential for the endonuclease of *EcoP*15I (Mackeldanz *et al*., 2013). Therefore, evidence suggests that the motif Q is more essential for classical helicases, but less or not essential for other helicase domain-containing proteins.

There are several potential roles for the Q motif. First, the Q motif may be involved in ATP binding. To be consistent with its initial findings by genetic and biochemical approaches (Tanner *et al*., 2003; Tanner, 2003), several crystal structures show that the Gln residue in Q motif interacts with ATP. For example in SF2 UvrB helicase, the Gln residue is mainly interacting with the adenine base positioning it for catalysis (Theis *et al*., 1999). Similarly, the Gln residue of an *E. coli* RecQ helicase (Bernstein and Keck, 2003) or archaeal XPD (Liu *et al*., 2008; Fan *et al*., 2008) is also located in a RecA domain near the ATP binding cleft. In a recent study, the Q motif residues L665, R669 and Q672 in Bloom's syndrome helicases are proved crucial for conferring nucleotide triphosphate specificity (Newman *et al*., 2015). Second, the Q motif is involved in substrate binding. From our previous work on FANCJ (Wu *et al*., 2012b) and current work, the Q motif is involved in DNA binding. In the crystal structure of XPD solved in the presence of a small fragment of bound DNA, the Q-motif stabilizes the P-loop via hydrogen bonding also suggesting a role in nucleotide binding and positioning (Kuper *et al*., 2012). Third, the Q motif might be involved in both ATP and nucleic acid binding. The study of Ded1 helicase demonstrates that the Q motif not only regulates ATP binding and hydrolysis but also

regulates the affinity of the protein for RNA substrates (Cordin *et al.*, 2004). To address whether conformal change by ATP binding will affect its nucleic acids binding, we incubated ChlR1-WT with AMP-PNP, then DNA substrate, and found its DNA binding activity was reduced (**Fig. 4.5C**). Lastly, the Q motif might be involved in protein oligomerization. It has been shown that the oligomerization of human RECQ1 is mediated by both an N-terminal domain (residues 1–103) that bears the conserved Gln residue (amino acid 96) and a C-terminal Winged helix domain (Lucic *et al*., 2011). The co-crystal structure of archaeal Hel308 with a partial duplex DNA molecule placed the Q motif on the edge of RecA domain 1 near the cleft that is formed with RecA domain 2 (Buttner *et al*., 2007).

5.2 The Role of the Motif Q and Motif I in ATP Binding

Motif I, also known as Walker A motif or the P-loop (phosphate-binding loop), is a motif in helicases that is associated with nucleotide phosphate group binding. The most conserved sequence for motif I has the pattern of Gly-X_4-Gly-Lys-(Thr/Ser), whereas the P-loop or glycine-rich loops function by binding the phosphate groups of ATP. However, the role of motif I is not universally true. In some helicases, such as UvrD and eIF4A, motif I has been shown to be important for both catalysis and ATP binding (Rozen *et al*., 1989; Pause and Sonenberg, 1992; Sinha *et al*., 2009). In contrast, in other helicases, including yeast RAD3 and some SWI2/SNF2 helicase-like proteins, motif I has been primarily identified as being critical for catalysis, but not for ATP binding (Nongkhlaw *et al*., 2012; Sung *et al*., 1988).

For the Q motif, the crystal structures of several helicase and nucleotide complexes showed that the glutamine side chain directly binds the adenine base of the nucleotide via a bidentate hydrogen bond (Strohmeier *et al*., 2011). The crystal structure of UAP56 helicase indicated that the glutamine contacts the N6 and N7 positions of the adenine base of ATP (**Fig. 5.1**) (Cordin *et al*., 2004; Shi *et al*., 2004). Further, changing the conserved

glutamine to alanine in Ded1 protein resulted in lowered catalytic efficiency as well as reduced affinity for ATP. All evidence above demonstrated that the Q motif is responsible for ATP binding. However, in FANCJ helicase the Q motif mutant FANCJ-Q25A displays impaired DNA binding ability but normal ATP binding (Wu *et al*., 2012b). Also, the Q motif in SWI2/SNF2 protein is only responsible for ATP hydrolysis but not ATP binding (Nongkhlaw *et al*., 2012). But Nongkhlaw et al. used a truncated Active DNA-dependent ATPase Domain instead of full length protein. Also, even SWI2/SNF2 proteins have helicase domain, they are not typical helicases.

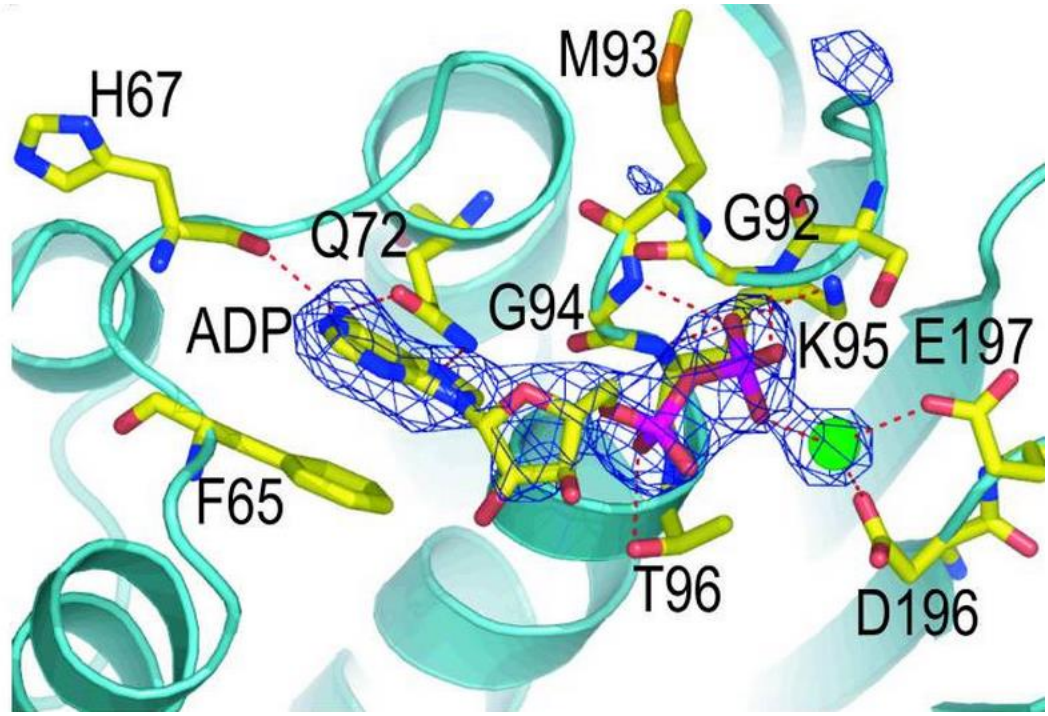

Fig. 5.1 A stereoview of UAP56–ADP interactions. The N6 and N7 atoms of the adenine base in ADP interact with the glutamine of the Q motif in UAP56 helicase (Q72). (From Shi *et al*., 2004. Reprinted with permission)

On the other hand, through Q motif's interactions with motif I and its importance for both ATP and RNA binding, it could act as a sensor for the state of the bound nucleotide. The Q motif could directly regulate the affinity of the protein for the substrate through conformational changes associated with nucleotide binding, and then regulate helicase activity. Also it could act as a regulator of ATPase activity; i.e., it activates hydrolysis of

ATP only when substrates are correctly bound to the protein (Cordin *et al*., 2004). The Q motif could stabilize a catalytically competent conformation of motif I and other helicase signature motifs (Strohmeier *et al*., 2011). They found that in Hera N-terminal domain, the Q motif mutant Q28E has an abnormal motif I conformation that is dictated by the mutated Q motif, which leads to the displacement of the phosphate moiety of bound nucleotides, and effectively abolishes the nucleotide-sensing capability of motif I. As a consequence, the relay of conformational changes that eventually lead to a closure of the cleft in the helicase core is blocked at the initial stage, which abrogates the unwinding activity of the protein (Strohmeier *et al*., 2011). In the ligand-free structures of eIF4A and BstDEAD, only a few interactions are seen between the Q motif and motif I (Carmel and Matthews, 2004; Story *et al*., 2001). However, this changes when a ligand is bound to motif I: in the ADP-bound eIF4A, in the MgADP-bound UAP56, in the sulfate-bound MjDEAD and in the citrate-bound UAP56, there are more extensive contacts between motif I and the Q motif (Story *et al*., 2001; Benz *et al*., 1999).

Therefore, it is still inconclusive whether motif Q and motif I function coordinately or independently. Further investigation is required. For example, mutagenesis analysis of motif Q, motif I , or both will shed light on their functions. Also changing glutamine to other amino acids, e.g., Q to N, Q to E, or Q to K, will help us to elucidate the structural roles of the Q motif. Moreover, structural determination of the Q motif with ATP or DNA will explain many pazzles that we have not answered.

5.3 The Q Motif is not Important for ATP Binding in ChlR1

Like ChlR1, FANCJ is also a member of the SF2 DEAH-box DNA helicase family (Wu *et al*., 2009). Previous work reported that the FANCJ-Q25A mutant can bind ATP as suggested by similar K_M values compared with the wild-type protein. However, the mutant protein is clearly compromised in its ability to hydrolyze ATP (Wu *et al*., 2012b). The reduced ATPase activity of FANCJ-Q25A may be partly attributed to its reduced ability

to bind DNA. Our current results also demonstrated that the ChlR1-Q23A mutant has poor DNA binding ability, suggesting that the role of the Q motif present in FANCJ and ChlR1 is involved in DNA binding. Since ATPase activity is usually DNA dependent, we hypothesize that the ChlR1-Q23A mutant abolished ATP hydrolysis activity due to its poor DNA binding ability.

In further ATP binding assays, we have used chromatography to determine how much ATP bound to ChlR1 proteins (**Fig. 4.8C** and **D**), and ATP-agarose beads to determine how much protein bound to ATP (**Fig. 4.9**). We also determined the equilibrium binding constant for ATP with a third method: filter dot blot. The k_d for ChlR1-WT and Q23A binding for ATP is 51.78 nM and 43.5 nM representatively (data not shown). All these results indicated that ChlR1-Q23A protein had normal ATP binding ability compared with ChlR1-WT. Thus, similar to the Q motif in FANCJ helicase, the Q motif in ChlR1 is not essential for ATP binding.

However, we cannot rule out other possibilities that the affect the protein's ATP hydrolysis activity. For example, ATP binds to protein, but not in a suitable conformation for hydrolysis to occur; or ATP binding causes a conformational change that inhibits the protein's DNA binding activity, which in turn reduces the protein's ATP hydrolysis activity; or ATP binding affects the protein's oligomerization state. Whether the Q motif in ChlR1 is directly involved in ATP binding can only be answered by co-crystallization of the ChlR1 protein with ATP.

5.4 ChlR1 Oligomerization and Potential Post-Translational Modification

DNA helicases appear to be generally oligomeric (usually dimers or hexamers), which provides the helicase with multiple DNA binding sites (Lohman and Bjornson, 1996) and this process can influence their catalytic or biological functions. Oligomerization is essential for ring-shaped helicases (RepA, Rho) to have function (Guo *et al*., 1999). Even though many helicases in non-ring-shaped SF1 and SF2 helicase function as monomers,

their activity is greatly enhanced by the formation of dimers or higher oligomers (Levin *et al*., 2004; Maluf *et al*., 2003; Tackett *et al*., 2005). The oligomerization state of ChlR1 is unknown, whereas biochemical studies have demonstrated that the optimal assembly state of FANCJ for catalytic activity is a dimer and the Q motif regulates its dimerization (Wu *et al*., 2012b). taXPD is believed to exist as a monomer in solution (Pugh *et al*., 2008), whereas eukaryotic XPD is a stable component of the multi-subunit general transcription factor TF IIH complex (Egly and Coin, 2011). Thus it is important to examine the ChlR1 oligomerization state which may influence its substrate specificity or catalytic efficiency.

We have used gel-filtration to determine whether ChlR1 that was purified from human cells can oligomerize, and the Q motif mutation might affect oligomerization. We have found that ChlR1 protein elutes as a monomer peak with a corresponding molecular weight of 141 kDa, and helicase analysis showed this monomeric form has unwinding activity. In fact, another Rad3/XPD family member, archaeal XPD, functions as a monomer in solution to unwind dsDNA substrate, and has no known stable interactions with other proteins (Rudolf *et al.,* 2006). Thus, the human ChlR1 protein seems to exist and function as a monomer, however, we found higher-order oligomers in a bacterial expression system.

We have expressed and purified ChlR1 protein from *E.coli,* and found that its oligomerization state is different from the protein purified from human cells. In addition to monomers, ChlR1 protein also forms tetramers in solution. Moreover, helicase analysis with duplex fork substrate revealed that the bacterial expressed ChlR1 has lower helicase activity than the human cells expressed ChlR1. Interestingly, the tetramer form of ChlR1 has higher unwinding activity compared with the monomeric form of ChlR1. The high protein expression level of bacteria may caused the ChlR1-WT to form tetramer in solution. Also, the length of DNA substrate could affect the oligomerization state of helicases. Longer substrate can provide more binding sites for helicases and they may form oligomers on the substrate instead of solution. We continuely observed tetramers and monomers for the bacterial expressed ChlR1 protein, but due to limited time we haven’t repeated the

helicase assays. Also, we faced sever protein aggregation when we attempted to purify ChlR1-Q23A, and some times with WT as well. In the future, instead of only using SEC, we will use ion exchange chromatography in the protein purification.

As we know, the human cell line expression system has much better post-translational modification (PTM) compared with bacterial expression systems. PTM can promote protein folding, improve stability as well as regulating functions (Khoury *et al*., 2011). In fact, the molecular mass of ChlR1 from human cells is 141 kDa, which is much higher than the ChlR1 protein from *E.coli* (119 kDa), indicating there is more PTM occurring to ChlR1 protein that is expressed in human cells. Indeed, several acetylation sites have been found in the ChlR1 protein (Dr. Robert Brosh lab, unpublished). Our lab also found ChlR1 undergoes ubiquitination (unpublished data). Thus, we can't rule out the possibility that bacteria are not able to correctly modify the ChlR1 helicase after translation. Proteins that do not express in soluble form may not be modified or folded properly, or may precipitate within *E. coli* through formation of inclusion bodies (Graslund *et al*., 2008). In this study, the bacterial expressed ChlR1 protein couldn't be purified without sarkosyl, which was used to denature the protein in order to solubilize the inclusion bodies. The protein is perhaps re-structured during purification, but we ddidn't know whether ChlR1 was correctly folded or not. As described above, the bacteria expressed tetramer form of ChlR1 may be not correctly folded as human cells expressed monomer ChlR1. Nevertheless, further investigation would be required.

5.5 Insight into the Role of the Q Motif from Bacterial Helicases to Human ChlR1

Although helicases share similarities in their three-dimensional folds, particularly the two RecA-like domains (Subramanya *et al*., 1996; Singleton *et al*., 2000; Bird *et al*., 1998), human helicase and its bacterial counterpart may have subtle differences in structure/function. So far human Rad3/XPD protein structure has not been solved. A

structure of ChlR1 helicase analog, *Thermoplasma acidophilum* XPD (TaXPD), has been solved with a short DNA fragment (Kuper *et al*., 2012). Point mutation experiments revealed that there are several DNA binding residues (R59A, R88H, E107A, F133A, Y166A, K170A, F326A, Y425E, W549S, D582N, and R584E) in the TaXPD helicase; however, the conserved glutamine (Q8) of Q motif is far from the DNA binding region (**Fig. 5.2A,** PDB 4A15).

In order to obtain insight into the structural function of the Q motif in ChlR1 helicase, we performed the tertiary structure prediction for the ChlR1 by superimposing the human ChlR1 sequence on the TaXPD structure (PDB 4A15, **Fig. 5.2B**). The predicted ChlR1 model starts from Glu202 and TaXPD structure begins with Arg5. Since full-length ChlR1 has 906 amino acids while taXPD has only 620 amino acids, about 180 amino acids between motif I and motif Ia is missing in TaXPD sequence (**Fig. 5.2C**). Thus the Q23 residue of human ChlR1 cannot be located in the predicted ChlR1 model. From this point of view, the predicted ChlR1 model can't truly illustrate the function of the Q motif in ChlR1 helicase. Furthermore, secondary structure prediction revealed that the sequence between motif I and motif Ia in ChlR1 is able to form α-helix and β-sheet (**Fig. 5.2D**). It is possible that there is an unidentified accessory helicase domain located between motif I and

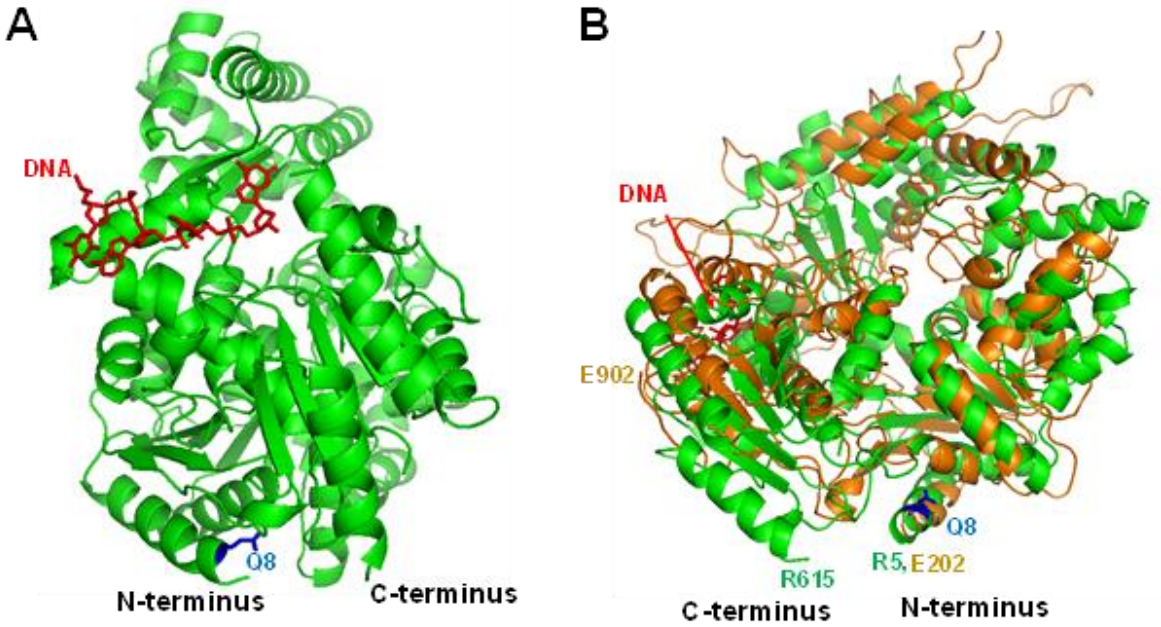

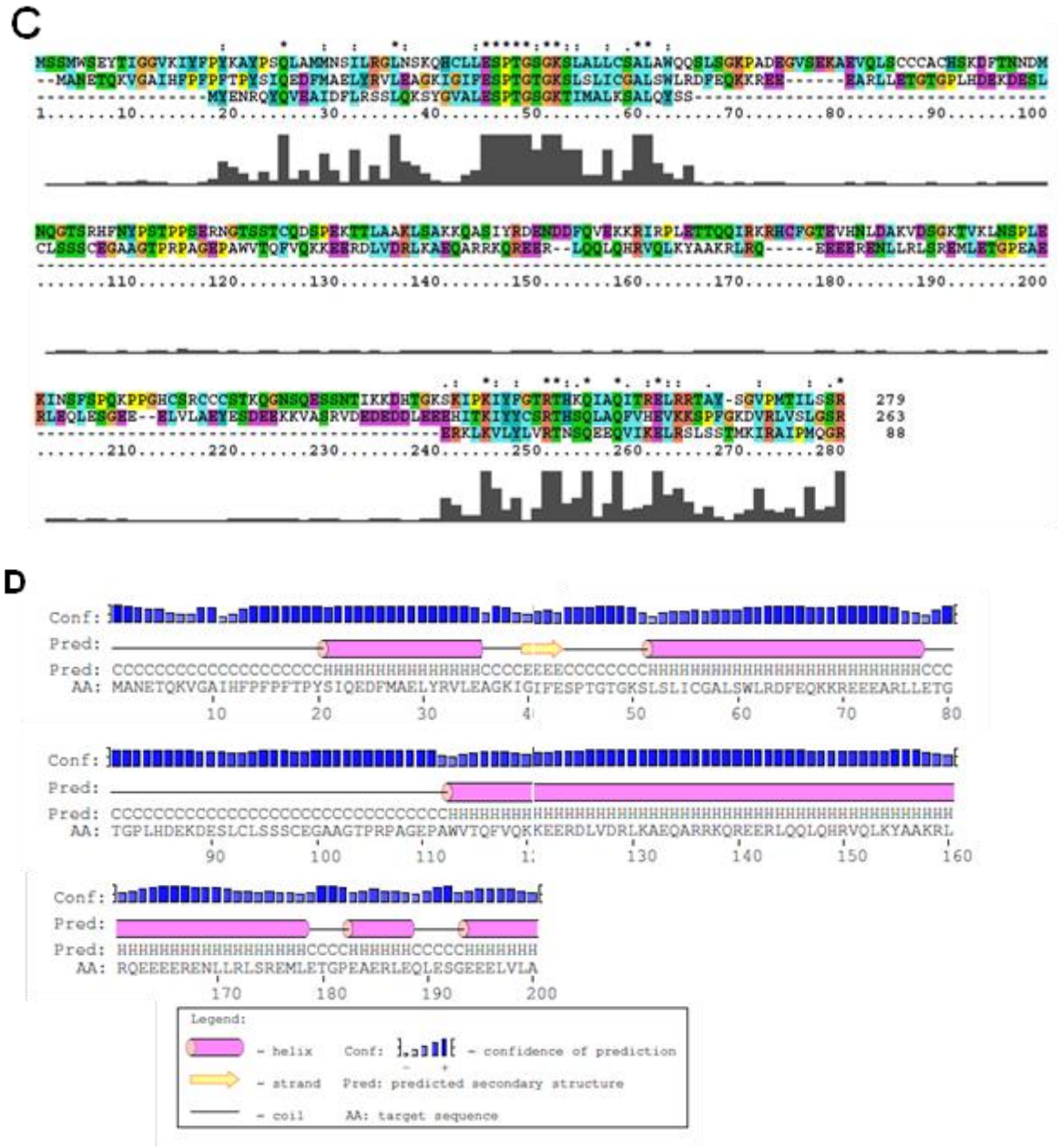

Fig. 5.2 ChlR1 secondary and tertiary structure prediction. (A) A side view of the TaXPD–DNA structure (PDB 4A15). Single-stranded DNA is indicated in red. The glutamine (Q8) is highlighted in blue. (B) Superimposing ChlR1 (orange) on a TaXPD helicase structure (green). The structure was made with program SWISS-MODE and viewed with Swiss PdbViewer 4.0. (C) Sequence alignment of the N terminal region of hsFANCJ (top), hsChlR1 (middle) and TaXPD (bottom). The grey bars indicate the homologous residues. The alignment was generated with Clustal X. (D) The secondary structure prediction for ChlR1 N terminus (1-200 aa). The pink columns represent α-helix, yellow arrows indicate β-sheet, and blue bar's heights indicate confidence of prediction. The secondary structure prediction was generated by PsiPred.

motif Ia. RTEL contains an accessory PIP domain which is capable of interacting with proliferating cell nuclear antigen (PCNA) (Warbrick, 2000). FANCJ contains an BRCA1 interacting accessory domain which is important for its DNA damage repair functions (Xie *et al*., 2010). Therefore we can't rule out the possibility that the Q motif in ChlR1 may have different structural functions, although the Q motif of TaXPD doesn't contact directly with single-stranded DNA. Also in a previous study, the Q motif in FANCJ helicase is involved in DNA binding (Wu *et al*., 2012b). Taken together, the exact roles of the Q motif in ChlR1 for ATP binding and/or DNA binding requires further investigation.

5.6 The Importance of the Q Motif in BLM and ChlR1 Helicases

Although ChlR1 Q motif mutations have not been found in patients, a missense mutation located in the Q motif (Q672R) in BLM helicase has been reported to cause Bloom syndrome (Ellis *et al*., 1995). The Bloom syndrome patient-derived BLM-Q672R mutation protein localized to the nucleus; however, there were a reduced number of foci after cellular exposure to mitomycin C or hydroxyurea (Guo *et al*., 2007). The BLM-Q672R mutation abolishes the helicase activity and severely diminishes the ATPase activity of the purified recombinant protein (Guo *et al*., 2007). However, the BLM-Q672R protein retained its normal DNA binding, leading the authors to propose that residue Gln-672 is involved in ATP binding. Although the Q23A mutation also impaired ChlR1 catalytic function, the effect of the mutation appears to be distinct from that of the BLM-Q672R mutation because the ChlR1-Q23A mutation impaired DNA binding. Overexpression of BLM-Q672R in Bloom syndrome cells failed to correct the high sister chromatid exchanges in Bloom syndrome cells (Neff *et al*., 1999), demonstrating that the molecular defect of the mutant protein displayed phenotypic consequences. ChlR1 is also involved in sister chromatid cohesion during mitosis, so it would be of interest to investigate the cellular functions of Q motif in ChlR1 helicase, such as a genetic complementation study will be required.

Recently, it was reported that ChlR1 is upregulated with progression from non-invasive to invasive melanoma, and is expressed at high levels in advanced melanoma (Bhattacharya *et al*., 2012). It is probable that ChlR1, like a number of DNA helicases, is differentially regulated in transformed or neoplastic cells and tissues in addition to melanoma (Brosh, Jr., 2013). It is still unknown why an increasing number of helicases are elicited to help cells deal with replication stress or DNA damage in cancer cells, and whether they are tailored to specific functions or tissue types. Indeed, early studies demonstrated that keratinocyte growth factor strongly induced the ChlR1 gene (Frank and Werner, 1996). ChlR1 may be a useful target for battling melanoma, but it is unclear what the consequence(s) of targeted ChlR1 inhibition would be for normal cells, or if other cancer cell types also rely on elevated ChlR1 expression for proliferation (Bhattacharya *et al*., 2012). Understanding the molecular and cellular functions of ChlR1 helicase should help us to better understanding the pathology of Warsaw breakage syndrome and melanoma.

6. Conclusions and Future Work

6.1 Conclusions

ChlR1-WT protein and ChlR1-Q23A mutant protein were successfully over-expressed, purified from HEK293T cells using FLAG antibody resin. We have discovered that the Q motif in ChlR1 is essential for its DNA binding, translocate and helicase activity. In other helicases, this conserved glutamine of the Q motif has been shown to be required for ATP binding, but we discovered that the Q motif is just essential for ATP hydrolysis instead of ATP binding in ChlR1 helicase. SEC results revealed that ChlR1-WT helicase function as monomer, which means the Q motif in ChlR1 is not involved in oligomerization. By using thermal shift assays and partial proteolysis mapping, we found that the globular structure of Q23A mutant protein is similar to wild-type protein, but subtle differences still exist. ChlR1-WT protein was also successfully expressed and extracted from bacterial with Ni-NTA chromatography. The bacterial expressed ChlR1-WT protein has different oligomerization state, monomer and tetramer were both observed in SEC profile. The tetramer form wild-type protein showed helicase activity on forked duplex substrate, but much lower when compared with HEK293T cell expressed protein.

Because all ChlR1-like helicases possess a Q motif, mutational analysis of the Q motif in ChlR1 helicases and related helicases will provide insight into the roles of the Q motif in superfamily 2 DNA helicases, which play vital roles in DNA replication, repair, recombination, and transcription.

6.2 Future Directions

The bacterial expressed ChlR1 protein is not soluble in solution until sarkosyl is added. Also ChlR1-Q23A protein aggregated during purification. The expression conditions and purification procedures need to be optimized. We can change the His tag into GST tag in order to make the protein more soluble. Or we can can try other tags like Arg-tag and Strep-tag. On the other hand, after the protein was unfolded by sarkosyl, the renature

process is incorrect and leaded to aggregation, so we should change the protein denature detergent.

Whether the motif Q function independently or coordinately with other motifs is still in conclusive, further investigation is required. Mutagenesis analysis of motif Q or other motifs will shed light on their functions. Also changing the glutamine of the motif Q to other amino acids, e.g., Q to N, Q to E, or Q to K, will help us to elucidate the structural roles of the Q motif.

The *in vivo* functions of ChlR1 protein haven't been determined. By transfecting GFP tagged ChlR1-WT or Q23A protein inside cells, we can detect whether DNA damage can induced foci in cells. Also, we are able to determine whether ChlR1-Q23A can function *in vivo* by genetic complementation of ChlR1-null cells, using sister chromatid cohesion as a readout.

7. References

Abdel-Monem,M., Durwald,H., and Hoffmann-Berling,H. (1976). Enzymic unwinding of DNA. 2. Chain separation by an ATP-dependent DNA unwinding enzyme. Eur. J. Biochem. *65*, 441-449.

Amaratunga,M. and Lohman,T.M. (1993). Escherichia coli rep helicase unwinds DNA by an active mechanism. Biochemistry. *32*, 6815-6820.

Astumian,R.D. (1997). Thermodynamics and kinetics of a Brownian motor. Science. *276*, 917-922.

Bailey,C., Fryer,A.E., and Greenslade,M. (2015). Warsaw Breakage Syndrome - A further report, emphasising cutaneous findings. Eur. J. Med. Genet. *19. S1769-7212*, 10.

Ballew,B.J., Joseph,V., De,S., Sarek,G., Vannier,J.B., Stracker,T., Schrader,K.A., Small,T.N., O'Reilly,R., Manschreck,C., Harlan Fleischut,M.M., Zhang,L., Sullivan,J., Stratton,K., Yeager,M., Jacobs,K., Giri,N., Alter,B.P., Boland,J., Burdett,L., Offit,K., Boulton,S.J., Savage,S.A., and Petrini,J.H. (2013). A recessive founder mutation in regulator of telomere elongation helicase 1, RTEL1, underlies severe immunodeficiency and features of Hoyeraal Hreidarsson syndrome. PLoS. Genet. *9*, e1003695.

Banroques,J., Cordin,O., Doere,M., Linder,P., and Tanner,N.K. (2011). Analyses of the functional regions of DEAD-box RNA "helicases" with deletion and chimera constructs tested in vivo and in vitro. J Mol Biol. *413*, 451-472.

Bennett,R.J. and Keck,J.L. (2004). Structure and function of RecQ DNA helicases. Crit Rev. Biochem. Mol. Biol. *39*, 79-97.

Benz,J., Trachsel,H., and Baumann,U. (1999). Crystal structure of the ATPase domain of translation initiation factor 4A from Saccharomyces cerevisiae--the prototype of the DEAD box protein family. Structure. *7*, 671-679.

Bernstein,D.A. and Keck,J.L. (2003). Domain mapping of Escherichia coli RecQ defines the roles of conserved N- and C-terminal regions in the RecQ family. Nucleic Acids Res. *31*, 2778-2785.

Bernstein,D.A., Zittel,M.C., and Keck,J.L. (2003). High-resolution structure of the E.coli RecQ helicase catalytic core. EMBO J. *22*, 4910-4921.

Bernstein,K.A., Gangloff,S., and Rothstein,R. (2010). The RecQ DNA helicases in DNA repair. Annu. Rev. Genet. *44*, 393-417.

Bhattacharya,C., Wang,X., and Becker,D. (2012). The DEAD/DEAH box helicase, DDX11,

is essential for the survival of advanced melanomas. Mol. Cancer. *11:82. doi: 10.1186/1476*, 82-11.

Biebricher,A., Hirano,S., Enzlin,J.H., Wiechens,N., Streicher,W.W., Huttner,D., Wang,L.H., Nigg,E.A., Owen-Hughes,T., Liu,Y., Peterman,E., Wuite,G.J., and Hickson,I.D. (2013). PICH: a DNA translocase specially adapted for processing anaphase bridge DNA. Mol. Cell. *51*, 691-701.

Bird,L.E., Subramanya,H.S., and Wigley,D.B. (1998). Helicases: a unifying structural theme? Curr. Opin. Struct. Biol. *8*, 14-18.

Boussif,O., Lezoualc'h,F., Zanta,M.A., Mergny,M.D., Scherman,D., Demeneix,B., and Behr,J.P. (1995). A versatile vector for gene and oligonucleotide transfer into cells in culture and in vivo: polyethylenimine. Proc. Natl. Acad. Sci. U. S. A. *92*, 7297-7301.

Brosh,R.M., Jr. (2013). DNA helicases involved in DNA repair and their roles in cancer. Nat. Rev. Cancer. *13*, 542-558.

Brosh,R.M., Jr. and Bohr,V.A. (2007). Human premature aging, DNA repair and RecQ helicases. Nucleic Acids Res. *35*, 7527-7544.

Brosh,R.M., Jr., Majumdar,A., Desai,S., Hickson,I.D., Bohr,V.A., and Seidman,M.M. (2001). Unwinding of a DNA triple helix by the Werner and Bloom syndrome helicases. J. Biol. Chem. *276*, 3024-3030.

Buttner,K., Nehring,S., and Hopfner,K.P. (2007). Structural basis for DNA duplex separation by a superfamily-2 helicase. Nat. Struct Mol Biol. *14*, 647-652.

Byrd,A.K. and Raney,K.D. (2005). Increasing the length of the single-stranded overhang enhances unwinding of duplex DNA by bacteriophage T4 Dda helicase. Biochemistry. *44*, 12990-12997.

Byrd,A.K. and Raney,K.D. (2012). Superfamily 2 helicases. Front Biosci. (Landmark. Ed). *17*, 2070-2088.

Cantor,S.B., Bell,D.W., Ganesan,S., Kass,E.M., Drapkin,R., Grossman,S., Wahrer,D.C., Sgroi,D.C., Lane,W.S., Haber,D.A., and Livingston,D.M. (2001). BACH1, a novel helicase-like protein, interacts directly with BRCA1 and contributes to its DNA repair function. Cell. *105*, 149-160.

Capo-Chichi,J.M., Bharti,S.K., Sommers,J.A., Yammine,T., Chouery,E., Patry,L., Rouleau,G.A., Samuels,M.E., Hamdan,F.F., Michaud,J.L., Brosh,R.M., Jr., Megarbane,A., and Kibar,Z. (2013). Identification and biochemical characterization of a novel mutation in DDX11 causing Warsaw breakage syndrome. Hum. Mutat. *34*, 103-107.

Carmel,A.B. and Matthews,B.W. (2004). Crystal structure of the BstDEAD N-terminal domain: a novel DEAD protein from Bacillus stearothermophilus. RNA. *10*, 66-74.

Cavlar,T., Deimling,T., Ablasser,A., Hopfner,K.P., and Hornung,V. (2013). Species-specific detection of the antiviral small-molecule compound CMA by STING. EMBO J. *32*, 1440-1450.

Cheng,W., Brendza,K.M., Gauss,G.H., Korolev,S., Waksman,G., and Lohman,T.M. (2002). The 2B domain of the Escherichia coli Rep protein is not required for DNA helicase activity. Proc. Natl. Acad. Sci. U. S. A. *99*, 16006-16011.

Cheng,W., Hsieh,J., Brendza,K.M., and Lohman,T.M. (2001). E. coli Rep oligomers are required to initiate DNA unwinding in vitro. J. Mol. Biol. *310*, 327-350.

Cordin,O., Tanner,N.K., Doere,M., Linder,P., and Banroques,J. (2004). The newly discovered Q motif of DEAD-box RNA helicases regulates RNA-binding and helicase activity. EMBO J. *23*, 2478-2487.

Del,C.M. and Lambowitz,A.M. (2009). Structure of the Yeast DEAD box protein Mss116p reveals two wedges that crimp RNA. Mol. Cell. *35*, 598-609.

DiGiovanna,J.J. and Kraemer,K.H. (2012). Shining a light on xeroderma pigmentosum. J. Invest Dermatol. *132*, 785-796.

Dillingham,M.S. (2011). Superfamily I helicases as modular components of DNA-processing machines. Biochem. Soc. Trans. *39*, 413-423.

Egly,J.M. and Coin,F. (2011). A history of TFIIH: two decades of molecular biology on a pivotal transcription/repair factor. DNA Repair (Amst). *10*, 714-721.

Ellis,N.A. (1997). DNA helicases in inherited human disorders. Curr. Opin. Genet. Dev. *7*, 354-363.

Ellis,N.A., Groden,J., Ye,T.Z., Straughen,J., Lennon,D.J., Ciocci,S., Proytcheva,M., and German,J. (1995). The Bloom's syndrome gene product is homologous to RecQ helicases. Cell. *83*, 655-666.

Fairman-Williams,M.E., Guenther,U.P., and Jankowsky,E. (2010). SF1 and SF2 helicases: family matters. Curr. Opin. Struct. Biol. *20*, 313-324.

Fan,L., Fuss,J.O., Cheng,Q.J., Arvai,A.S., Hammel,M., Roberts,V.A., Cooper,P.K., and Tainer,J.A. (2008). XPD helicase structures and activities: insights into the cancer and aging phenotypes from XPD mutations. Cell. *133*, 789-800.

Fang,J., Acheampong,E., Dave,R., Wang,F., Mukhtar,M., and Pomerantz,R.J. (2005). The

RNA helicase DDX1 is involved in restricted HIV-1 Rev function in human astrocytes. Virology. *336*, 299-307.

Farina,A., Shin,J.H., Kim,D.H., Bermudez,V.P., Kelman,Z., Seo,Y.S., and Hurwitz,J. (2008). Studies with the human cohesin establishment factor, ChlR1. Association of ChlR1 with Ctf18-RFC and Fen1. J. Biol. Chem. *283*, 20925-20936.

Fontana,A., de Laureto,P.P., Spolaore,B., Frare,E., Picotti,P., and Zambonin,M. (2004). Probing protein structure by limited proteolysis. Acta Biochim. Pol. *51*, 299-321.

Frank,S. and Werner,S. (1996). The human homologue of the yeast CHL1 gene is a novel keratinocyte growth factor-regulated gene. J. Biol. Chem. *271*, 24337-24340.

Fuller-Pace,F.V. (2006). DExD/H box RNA helicases: multifunctional proteins with important roles in transcriptional regulation. Nucleic Acids Res. *34*, 4206-4215.

Gallivan,J.P. and McGarvey,M.J. (2003). The importance of the Q motif in the ATPase activity of a viral helicase. FEBS Lett. *20;554*, 485-488.

Giglia-Mari,G., Coin,F., Ranish,J.A., Hoogstraten,D., Theil,A., Wijgers,N., Jaspers,N.G., Raams,A., Argentini,M., van der Spek,P.J., Botta,E., Stefanini,M., Egly,J.M., Aebersold,R., Hoeijmakers,J.H., and Vermeulen,W. (2004). A new, tenth subunit of TFIIH is responsible for the DNA repair syndrome trichothiodystrophy group A. Nat. Genet. *36*, 714-719.

Gilhooly,N.S. and Dillingham,M.S. (2014). Recombination hotspots attenuate the coupled ATPase and translocase activities of an AddAB-type helicase-nuclease. Nucleic Acids Res. *42*, 5633-5643.

Graslund,S., Nordlund,P., Weigelt,J., Hallberg,B.M., Bray,J., Gileadi,O., Knapp,S., Oppermann,U., Arrowsmith,C., Hui,R., Ming,J., dhe-Paganon,S., Park,H.W., Savchenko,A., Yee,A., Edwards,A., Vincentelli,R., Cambillau,C., Kim,R., Kim,S.H., Rao,Z., Shi,Y., Terwilliger,T.C., Kim,C.Y., Hung,L.W., Waldo,G.S., Peleg,Y., Albeck,S., Unger,T., Dym,O., Prilusky,J., Sussman,J.L., Stevens,R.C., Lesley,S.A., Wilson,I.A., Joachimiak,A., Collart,F., Dementieva,I., Donnelly,M.I., Eschenfeldt,W.H., Kim,Y., Stols,L., Wu,R., Zhou,M., Burley,S.K., Emtage,J.S., Sauder,J.M., Thompson,D., Bain,K., Luz,J., Gheyi,T., Zhang,F., Atwell,S., Almo,S.C., Bonanno,J.B., Fiser,A., Swaminathan,S., Studier,F.W., Chance,M.R., Sali,A., Acton,T.B., Xiao,R., Zhao,L., Ma,L.C., Hunt,J.F., Tong,L., Cunningham,K., Inouye,M., Anderson,S., Janjua,H., Shastry,R., Ho,C.K., Wang,D., Wang,H., Jiang,M., Montelione,G.T., Stuart,D.I., Owens,R.J., Daenke,S., Schutz,A., Heinemann,U., Yokoyama,S., Bussow,K., and Gunsalus,K.C. (2008). Protein production and purification. Nat. Methods. *5*, 135-146.

Guo,M., Hundseth,K., Ding,H., Vidhyasagar,V., Inoue,A., Nguyen,C.H., Zain,R., Lee,J.S., and Wu,Y. (2015). A Distinct Triplex DNA Unwinding Activity of ChlR1 Helicase. J. Biol.

Chem. *20;290*, 5174-5189.

Guo,R.B., Rigolet,P., Ren,H., Zhang,B., Zhang,X.D., Dou,S.X., Wang,P.Y., Amor-Gueret,M., and Xi,X.G. (2007). Structural and functional analyses of disease-causing missense mutations in Bloom syndrome protein. Nucleic Acids Res. *35*, 6297-6310.

Guo,S., Tabor,S., and Richardson,C.C. (1999). The linker region between the helicase and primase domains of the bacteriophage T7 gene 4 protein is critical for hexamer formation. J. Biol. Chem. *274*, 30303-30309.

Guzder,S.N., Qiu,H., Sommers,C.H., Sung,P., Prakash,L., and Prakash,S. (1994). DNA repair gene RAD3 of S. cerevisiae is essential for transcription by RNA polymerase II. Nature. *367*, 91-94.

Hajer,B.H., Dorra,Z.A., Monia,M., Samir,B., and Nushin,A. (2014). Probing the role of helix alpha1 in the acid-tolerance and thermal stability of the Streptomyces sp. SK Glucose Isomerase by site-directed mutagenesis. J. Biotechnol. *173:Epub;2014 Jan 15.*, 1-6.

Hilbert,M., Karow,A.R., and Klostermeier,D. (2009). The mechanism of ATP-dependent RNA unwinding by DEAD box proteins. Biol. Chem. *390*, 1237-1250.

Hill,T.L. and Tsuchiya,T. (1981). Theoretical aspects of translocation on DNA: adenosine triphosphatases and treadmilling binding proteins. Proc. Natl. Acad. Sci. U. S. A. *78*, 4796-4800.

Hirota,Y. and Lahti,J.M. (2000). Characterization of the enzymatic activity of hChlR1, a novel human DNA helicase. Nucleic Acids Res. *28*, 917-924.

Inoue,A., Li,T., Roby,S.K., Valentine,M.B., Inoue,M., Boyd,K., Kidd,V.J., and Lahti,J.M. (2007). Loss of ChlR1 helicase in mouse causes lethality due to the accumulation of aneuploid cells generated by cohesion defects and placental malformation. Cell Cycle. *6*, 1646-1654.

Jankowsky,E. (2011). RNA helicases at work: binding and rearranging. Trends Biochem. Sci. *36*, 19-29.

Jankowsky,E. and Bowers,H. (2006). Remodeling of ribonucleoprotein complexes with DExH/D RNA helicases. Nucleic Acids Res. *34*, 4181-4188.

Jankowsky,E. and Fairman,M.E. (2007). RNA helicases--one fold for many functions. Curr. Opin. Struct. Biol. *17*, 316-324.

Jarmoskaite,I. and Russell,R. (2014). RNA helicase proteins as chaperones and remodelers. Annu. Rev. Biochem. *83. Epub;2014 Mar 12.*, 697-725.

Jezewska,M.J., Rajendran,S., and Bujalowski,W. (1998). Complex of Escherichia coli primary replicative helicase DnaB protein with a replication fork: recognition and structure. Biochemistry. *37*, 3116-3136.

Kaplan,D.L. (2000). The 3'-tail of a forked-duplex sterically determines whether one or two DNA strands pass through the central channel of a replication-fork helicase. J. Mol. Biol. *301*, 285-299.

Kaplan,D.L., Davey,M.J., and O'Donnell,M. (2003). Mcm4,6,7 uses a "pump in ring" mechanism to unwind DNA by steric exclusion and actively translocate along a duplex. J. Biol. Chem. *278*, 49171-49182.

Kawaoka,J., Jankowsky,E., and Pyle,A.M. (2004). Backbone tracking by the SF2 helicase NPH-II. Nat. Struct. Mol. Biol. *11*, 526-530.

Khoury,G.A., Baliban,R.C., and Floudas,C.A. (2011). Proteome-wide post-translational modification statistics: frequency analysis and curation of the swiss-prot database. Sci. Rep. *1. pii: srep00090.*.

Klostermeier,D. and Rudolph,M.G. (2009). A novel dimerization motif in the C-terminal domain of the Thermus thermophilus DEAD box helicase Hera confers substantial flexibility. Nucleic Acids Res. *37*, 421-430.

Kuper,J., Wolski,S.C., Michels,G., and Kisker,C. (2012). Functional and structural studies of the nucleotide excision repair helicase XPD suggest a polarity for DNA translocation. EMBO J. *31*, 494-502.

Lamberti,A., Longo,O., Del,V.P., Zambrano,N., Barone,G., Russo,T., and Arcari,P. (2005). Probing the secondary structure of a recombinant neuronal adaptor protein and its phosphotyrosine binding domains. Biosci. Biotechnol. Biochem. *69*, 2395-2400.

Le,G.T., Jullien,L., Touzot,F., Schertzer,M., Gaillard,L., Perderiset,M., Carpentier,W., Nitschke,P., Picard,C., Couillault,G., Soulier,J., Fischer,A., Callebaut,I., Jabado,N., Londono-Vallejo,A., de Villartay,J.P., and Revy,P. (2013). Human RTEL1 deficiency causes Hoyeraal-Hreidarsson syndrome with short telomeres and genome instability. Hum. Mol. Genet. *22*, 3239-3249.

Lee,J.Y. and Yang,W. (2006). UvrD helicase unwinds DNA one base pair at a time by a two-part power stroke. Cell. *127*, 1349-1360.

Lehmann,A.R. (2003). DNA repair-deficient diseases, xeroderma pigmentosum, Cockayne syndrome and trichothiodystrophy. Biochimie. *85*, 1101-1111.

Leipe,D.D., Wolf,Y.I., Koonin,E.V., and Aravind,L. (2002). Classification and evolution of

P-loop GTPases and related ATPases. J. Mol. Biol. *317*, 41-72.

Leman,A.R., Noguchi,C., Lee,C.Y., and Noguchi,E. (2010). Human Timeless and Tipin stabilize replication forks and facilitate sister-chromatid cohesion. J. Cell Sci. *123*, 660-670.

Levin,M.K., Gurjar,M., and Patel,S.S. (2005). A Brownian motor mechanism of translocation and strand separation by hepatitis C virus helicase. Nat. Struct. Mol. Biol. *12*, 429-435.

Levin,M.K., Wang,Y.H., and Patel,S.S. (2004). The functional interaction of the hepatitis C virus helicase molecules is responsible for unwinding processivity. J. Biol. Chem. *279*, 26005-26012.

Levitus,M., Waisfisz,Q., Godthelp,B.C., de,V.Y., Hussain,S., Wiegant,W.W., Elghalbzouri-Maghrani,E., Steltenpool,J., Rooimans,M.A., Pals,G., Arwert,F., Mathew,C.G., Zdzienicka,M.Z., Hiom,K., de Winter,J.P., and Joenje,H. (2005). The DNA helicase BRIP1 is defective in Fanconi anemia complementation group J. Nat. Genet. *37*, 934-935.

Levran,O., Attwooll,C., Henry,R.T., Milton,K.L., Neveling,K., Rio,P., Batish,S.D., Kalb,R., Velleuer,E., Barral,S., Ott,J., Petrini,J., Schindler,D., Hanenberg,H., and Auerbach,A.D. (2005). The BRCA1-interacting helicase BRIP1 is deficient in Fanconi anemia. Nat. Genet. *37*, 931-933.

Litman,R., Peng,M., Jin,Z., Zhang,F., Zhang,J., Powell,S., Andreassen,P.R., and Cantor,S.B. (2005). BACH1 is critical for homologous recombination and appears to be the Fanconi anemia gene product FANCJ. Cancer Cell. *8*, 255-265.

Liu,H., Rudolf,J., Johnson,K.A., McMahon,S.A., Oke,M., Carter,L., McRobbie,A.M., Brown,S.E., Naismith,J.H., and White,M.F. (2008). Structure of the DNA repair helicase XPD. Cell. *133*, 801-812.

Lohman,T.M. and Bjornson,K.P. (1996). Mechanisms of helicase-catalyzed DNA unwinding. Annu. Rev. Biochem. *65:169-214.*.

Lucic,B., Zhang,Y., King,O., Mendoza-Maldonado,R., Berti,M., Niesen,F.H., Burgess-Brown,N.A., Pike,A.C., Cooper,C.D., Gileadi,O., and Vindigni,A. (2011). A prominent beta-hairpin structure in the winged-helix domain of RECQ1 is required for DNA unwinding and oligomer formation. Nucleic Acids Res. *39*, 1703-1717.

Lusser,A. and Kadonaga,J.T. (2003). Chromatin remodeling by ATP-dependent molecular machines. Bioessays. *25*, 1192-1200.

Mackeldanz,P., Alves,J., Moncke-Buchner,E., Wyszomirski,K.H., Kruger,D.H., and Reuter,M. (2013). Functional consequences of mutating conserved SF2 helicase motifs in

the Type III restriction endonuclease EcoP15I translocase domain. Biochimie. *95*, 817-823.

Mackintosh,S.G. and Raney,K.D. (2006). DNA unwinding and protein displacement by superfamily 1 and superfamily 2 helicases. Nucleic Acids Res. *34*, 4154-4159.

Maizels,N. (2006). Dynamic roles for G4 DNA in the biology of eukaryotic cells. Nat. Struct. Mol. Biol. *13*, 1055-1059.

Maluf,N.K., Fischer,C.J., and Lohman,T.M. (2003). A Dimer of Escherichia coli UvrD is the active form of the helicase in vitro. J. Mol. Biol. *325*, 913-935.

Manosas,M., Xi,X.G., Bensimon,D., and Croquette,V. (2010). Active and passive mechanisms of helicases. Nucleic Acids Res. *38*, 5518-5526.

Manthei,K.A., Hill,M.C., Burke,J.E., Butcher,S.E., and Keck,J.L. (2015). Structural mechanisms of DNA binding and unwinding in bacterial RecQ helicases. Proc. Natl. Acad. Sci. U. S. A. *112*, 4292-4297.

Mayer,M.L., Pot,I., Chang,M., Xu,H., Aneliunas,V., Kwok,T., Newitt,R., Aebersold,R., Boone,C., Brown,G.W., and Hieter,P. (2004). Identification of protein complexes required for efficient sister chromatid cohesion. Mol. Biol. Cell. *15*, 1736-1745.

McClelland,S.E., Dryden,D.T., and Szczelkun,M.D. (2005). Continuous assays for DNA translocation using fluorescent triplex dissociation: application to type I restriction endonucleases. J. Mol. Biol. *348*, 895-915.

Meetei,A.R., Medhurst,A.L., Ling,C., Xue,Y., Singh,T.R., Bier,P., Steltenpool,J., Stone,S., Dokal,I., Mathew,C.G., Hoatlin,M., Joenje,H., de Winter,J.P., and Wang,W. (2005). A human ortholog of archaeal DNA repair protein Hef is defective in Fanconi anemia complementation group M. Nat. Genet. *37*, 958-963.

Nanduri,B., Byrd,A.K., Eoff,R.L., Tackett,A.J., and Raney,K.D. (2002). Pre-steady-state DNA unwinding by bacteriophage T4 Dda helicase reveals a monomeric molecular motor. Proc. Natl. Acad. Sci. U. S. A. *99*, 14722-14727.

Neff,N.F., Ellis,N.A., Ye,T.Z., Noonan,J., Huang,K., Sanz,M., and Proytcheva,M. (1999). The DNA helicase activity of BLM is necessary for the correction of the genomic instability of bloom syndrome cells. Mol. Biol. Cell. *10*, 665-676.

Newman,J.A., Savitsky,P., Allerston,C.K., Bizard,A.H., Ozer,O., Sarlos,K., Liu,Y., Pardon,E., Steyaert,J., Hickson,I.D., and Gileadi,O. (2015). Crystal structure of the Bloom's syndrome helicase indicates a role for the HRDC domain in conformational changes. Nucleic Acids Res. *43*, 5221-5235.

Nongkhlaw,M., Gupta,M., Komath,S.S., and Muthuswami,R. (2012). Motifs Q and I are required for ATP hydrolysis but not for ATP binding in SWI2/SNF2 proteins. Biochemistry. *51*, 3711-3722.

Parish,J.L., Rosa,J., Wang,X., Lahti,J.M., Doxsey,S.J., and Androphy,E.J. (2006). The DNA helicase ChlR1 is required for sister chromatid cohesion in mammalian cells. J. Cell Sci. *119*, 4857-4865.

Parsyan,A., Svitkin,Y., Shahbazian,D., Gkogkas,C., Lasko,P., Merrick,W.C., and Sonenberg,N. (2011). mRNA helicases: the tacticians of translational control. Nat. Rev. Mol. Cell Biol. *12*, 235-245.

Patel,S.S. and Donmez,I. (2006). Mechanisms of helicases. J. Biol. Chem. *281*, 18265-18268.

Patel,S.S. and Picha,K.M. (2000). Structure and function of hexameric helicases. Annu. Rev. Biochem. *69:651-97.*.

Pause,A. and Sonenberg,N. (1992). Mutational analysis of a DEAD box RNA helicase: the mammalian translation initiation factor eIF-4A. EMBO J. *11*, 2643-2654.

Pugh,R.A., Honda,M., Leesley,H., Thomas,A., Lin,Y., Nilges,M.J., Cann,I.K., and Spies,M. (2008). The iron-containing domain is essential in Rad3 helicases for coupling of ATP hydrolysis to DNA translocation and for targeting the helicase to the single-stranded DNA-double-stranded DNA junction. J. Biol. Chem. *283*, 1732-1743.

Pyle,A.M. (2008). Translocation and unwinding mechanisms of RNA and DNA helicases. Annu. Rev. Biophys. *37:* 317-336.

Robertson-Anderson,R.M., Wang,J., Edgcomb,S.P., Carmel,A.B., Williamson,J.R., and Millar,D.P. (2011). Single-molecule studies reveal that DEAD box protein DDX1 promotes oligomerization of HIV-1 Rev on the Rev response element. J. Mol. Biol. *410*, 959-971.

Rozen,F., Pelletier,J., Trachsel,H., and Sonenberg,N. (1989). A lysine substitution in the ATP-binding site of eucaryotic initiation factor 4A abrogates nucleotide-binding activity. Mol. Cell Biol. *9*, 4061-4063.

Rudolf,J., Makrantoni,V., Ingledew,W.J., Stark,M.J., and White,M.F. (2006). The DNA repair helicases XPD and FancJ have essential iron-sulfur domains. Mol. Cell. *23*, 801-808.

Rudra,S. and Skibbens,R.V. (2012). Sister chromatid cohesion establishment occurs in concert with lagging strand synthesis. Cell Cycle. *11*, 2114-2121.

Rudra,S. and Skibbens,R.V. (2013). Chl1 DNA helicase regulates Scc2 deposition

specifically during DNA-replication in Saccharomyces cerevisiae. PLoS. One. *8*, e75435.

Sainsbury,S., Bird,L., Rao,V., Shepherd,S.M., Stuart,D.I., Hunter,W.N., Owens,R.J., and Ren,J. (2011). Crystal structures of penicillin-binding protein 3 from Pseudomonas aeruginosa: comparison of native and antibiotic-bound forms. J. Mol. Biol. *405*, 173-184.

Schlee,M., Roth,A., Hornung,V., Hagmann,C.A., Wimmenauer,V., Barchet,W., Coch,C., Janke,M., Mihailovic,A., Wardle,G., Juranek,S., Kato,H., Kawai,T., Poeck,H., Fitzgerald,K.A., Takeuchi,O., Akira,S., Tuschl,T., Latz,E., Ludwig,J., and Hartmann,G. (2009). Recognition of 5' triphosphate by RIG-I helicase requires short blunt double-stranded RNA as contained in panhandle of negative-strand virus. Immunity. *31*, 25-34.

Shah,N., Inoue,A., Woo,L.S., Beishline,K., Lahti,J.M., and Noguchi,E. (2013). Roles of ChlR1 DNA helicase in replication recovery from DNA damage. Exp. Cell Res. *319*, 2244-2253.

Shi,H., Cordin,O., Minder,C.M., Linder,P., and Xu,R.M. (2004). Crystal structure of the human ATP-dependent splicing and export factor UAP56. Proc. Natl. Acad. Sci. U. S. A. *101*, 17628-17633.

Siitonen,H.A., Kopra,O., Kaariainen,H., Haravuori,H., Winter,R.M., Saamanen,A.M., Peltonen,L., and Kestila,M. (2003). Molecular defect of RAPADILINO syndrome expands the phenotype spectrum of RECQL diseases. Hum. Mol. Genet. *12*, 2837-2844.

Singh,D.K., Ghosh,A.K., Croteau,D.L., and Bohr,V.A. (2012). RecQ helicases in DNA double strand break repair and telomere maintenance. Mutat. Res. *736*, 15-24.

Singleton,M.R., Dillingham,M.S., and Wigley,D.B. (2007). Structure and mechanism of helicases and nucleic acid translocases. Annu. Rev. Biochem. *76:23-50.*.

Singleton,M.R., Sawaya,M.R., Ellenberger,T., and Wigley,D.B. (2000). Crystal structure of T7 gene 4 ring helicase indicates a mechanism for sequential hydrolysis of nucleotides. Cell. *101*, 589-600.

Sinha,K.M., Glickman,M.S., and Shuman,S. (2009). Mutational analysis of Mycobacterium UvrD1 identifies functional groups required for ATP hydrolysis, DNA unwinding, and chemomechanical coupling. Biochemistry. *19;48*, 4019-4030.

Skibbens,R.V. (2004). Chl1p, a DNA helicase-like protein in budding yeast, functions in sister-chromatid cohesion. Genetics. *166*, 33-42.

Soultanas,P. and Wigley,D.B. (2001). Unwinding the 'Gordian knot' of helicase action. Trends Biochem. Sci. *26*, 47-54.

Story,R.M., Li,H., and Abelson,J.N. (2001). Crystal structure of a DEAD box protein from the hyperthermophile Methanococcus jannaschii. Proc. Natl. Acad. Sci. U. S. A. *98*, 1465-1470.

Strohmeier,J., Hertel,I., Diederichsen,U., Rudolph,M.G., and Klostermeier,D. (2011). Changing nucleotide specificity of the DEAD-box helicase Hera abrogates communication between the Q-motif and the P-loop. Biol. Chem. *392*, 357-369.

Subramanya,H.S., Bird,L.E., Brannigan,J.A., and Wigley,D.B. (1996). Crystal structure of a DExx box DNA helicase. Nature. *384*, 379-383.

Sung,P., Guzder,S.N., Prakash,L., and Prakash,S. (1996). Reconstitution of TFIIH and requirement of its DNA helicase subunits, Rad3 and Rad25, in the incision step of nucleotide excision repair. J. Biol. Chem. *271*, 10821-10826.

Sung,P., Higgins,D., Prakash,L., and Prakash,S. (1988). Mutation of lysine-48 to arginine in the yeast RAD3 protein abolishes its ATPase and DNA helicase activities but not the ability to bind ATP. EMBO J. *7*, 3263-3269.

Svitkin,Y.V., Pause,A., Haghighat,A., Pyronnet,S., Witherell,G., Belsham,G.J., and Sonenberg,N. (2001). The requirement for eukaryotic initiation factor 4A (elF4A) in translation is in direct proportion to the degree of mRNA 5' secondary structure. RNA. *7*, 382-394.

Tackett,A.J., Chen,Y., Cameron,C.E., and Raney,K.D. (2005). Multiple full-length NS3 molecules are required for optimal unwinding of oligonucleotide DNA in vitro. J. Biol. Chem. *280*, 10797-10806.

Tackett,A.J., Morris,P.D., Dennis,R., Goodwin,T.E., and Raney,K.D. (2001). Unwinding of unnatural substrates by a DNA helicase. Biochemistry. *40*, 543-548.

Tanner,N.K. (2003). The newly identified Q motif of DEAD box helicases is involved in adenine recognition. Cell Cycle *2*, 18-19.

Tanner,N.K., Cordin,O., Banroques,J., Doere,M., and Linder,P. (2003). The Q motif: a newly identified motif in DEAD box helicases may regulate ATP binding and hydrolysis. Mol. Cell. *11*, 127-138.

Tanner,N.K. and Linder,P. (2001). DExD/H box RNA helicases: from generic motors to specific dissociation functions. Mol. Cell. *8*, 251-262.

Theis,K., Chen,P.J., Skorvaga,M., Van,H.B., and Kisker,C. (1999). Crystal structure of UvrB, a DNA helicase adapted for nucleotide excision repair. EMBO J. *18*, 6899-6907.

Trkulja,C.L., Jansson,E.T., Jardemark,K., and Orwar,O. (2014). Probing structure and function of ion channels using limited proteolysis and microfluidics. J. Am. Chem. Soc. *136*, 14875-14882.

Tsay,J.M., Sippy,J., Feiss,M., and Smith,D.E. (2009). The Q motif of a viral packaging motor governs its force generation and communicates ATP recognition to DNA interaction. Proc. Natl. Acad. Sci. U. S. A. *106*, 14355-14360.

van Brabant,A.J., Stan,R., and Ellis,N.A. (2000). DNA helicases, genomic instability, and human genetic disease. Annu. Rev. Genomics Hum. Genet. *1:409-59.*.

van der Lelij,P., Chrzanowska,K.H., Godthelp,B.C., Rooimans,M.A., Oostra,A.B., Stumm,M., Zdzienicka,M.Z., Joenje,H., and de Winter,J.P. (2010). Warsaw breakage syndrome, a cohesinopathy associated with mutations in the XPD helicase family member DDX11/ChlR1. Am. J. Hum. Genet. *86*, 262-266.

Velankar,S.S., Soultanas,P., Dillingham,M.S., Subramanya,H.S., and Wigley,D.B. (1999). Crystal structures of complexes of PcrA DNA helicase with a DNA substrate indicate an inchworm mechanism. Cell. *97*, 75-84.

Voloshin,O.N., Vanevski,F., Khil,P.P., and Camerini-Otero,R.D. (2003). Characterization of the DNA damage-inducible helicase DinG from Escherichia coli. J. Biol. Chem. *278*, 28284-28293.

von Hippel,P.H. and Delagoutte,E. (2001). A general model for nucleic acid helicases and their "coupling" within macromolecular machines. Cell. *104*, 177-190.

Warbrick,E. (2000). The puzzle of PCNA's many partners. Bioessays. *22*, 997-1006.

Wolski,S.C., Kuper,J., Hanzelmann,P., Truglio,J.J., Croteau,D.L., Van,H.B., and Kisker,C. (2008). Crystal structure of the FeS cluster-containing nucleotide excision repair helicase XPD. PLoS. Biol. *6*, e149.

Wong,I. and Lohman,T.M. (1992). Allosteric effects of nucleotide cofactors on Escherichia coli Rep helicase-DNA binding. Science. *256*, 350-355.

Worrall,J.A., Howe,F.S., McKay,A.R., Robinson,C.V., and Luisi,B.F. (2008). Allosteric activation of the ATPase activity of the Escherichia coli RhlB RNA helicase. J. Biol. Chem. *283*, 5567-5576.

Wu,Y. and Brosh,R.M., Jr. (2012). DNA helicase and helicase-nuclease enzymes with a conserved iron-sulfur cluster. Nucleic Acids Res. *40*, 4247-4260.

Wu,Y., Shin-ya,K., and Brosh,R.M., Jr. (2008). FANCJ helicase defective in Fanconia

anemia and breast cancer unwinds G-quadruplex DNA to defend genomic stability. Mol. Cell Biol. *28*, 4116-4128.

Wu,Y., Sommers,J.A., Khan,I., de Winter,J.P., and Brosh,R.M., Jr. (2012a). Biochemical characterization of Warsaw breakage syndrome helicase. J. Biol. Chem. *287*, 1007-1021.

Wu,Y., Sommers,J.A., Loiland,J.A., Kitao,H., Kuper,J., Kisker,C., and Brosh,R.M., Jr. (2012b). The Q motif of Fanconi anemia group J protein (FANCJ) DNA helicase regulates its dimerization, DNA binding, and DNA repair function. J. Biol. Chem. *287*, 21699-21716.

Wu,Y., Suhasini,A.N., and Brosh,R.M., Jr. (2009). Welcome the family of FANCJ-like helicases to the block of genome stability maintenance proteins. Cell Mol. Life Sci. *66*, 1209-1222.

Xie,J., Litman,R., Wang,S., Peng,M., Guillemette,S., Rooney,T., and Cantor,S.B. (2010). Targeting the FANCJ-BRCA1 interaction promotes a switch from recombination to poleta-dependent bypass. Oncogene. *29*, 2499-2508.

Xu,H.Q., Deprez,E., Zhang,A.H., Tauc,P., Ladjimi,M.M., Brochon,J.C., Auclair,C., and Xi,X.G. (2003). The Escherichia coli RecQ helicase functions as a monomer. J. Biol. Chem. *278*, 34925-34933.

Yarranton,G.T. and Gefter,M.L. (1979). Enzyme-catalyzed DNA unwinding: studies on Escherichia coli rep protein. Proc. Natl. Acad. Sci. U. S. A. *76*, 1658-1662.

Yu,J., Ha,T., and Schulten,K. (2006). Structure-based model of the stepping motor of PcrA helicase. Biophys. J. *91*, 2097-2114.